# RESEARCH AND DEVELOPMENT ON DISCONTINUOUS FIBER REINFORCED LIGHT ALLOYS

March 1971-March 1972

FINAL REPORT

by
R. A. Hermann
P. J. Lare
F. Ordway
H. Hahn

Prepared for

DEPARTMENT OF THE NAVY
Naval Ordnance Systems Command
Washington, D.C. 20360

Contract No. N00017-71-C-4404

Submitted by
ARTECH CORP.
2816 Fallfax Drive
Falls Church, Virginia 22042

7016-FR

57

## DOCUMENT CONTROL DATA - R & D

*(Security classification of title, body of abstract and indexing annotation must be entered when the overall report is classified)*

1. ORIGINATING ACTIVITY (Corporate author)
ARTECH CORP.
2816 Fallfax Drive
Falls Church, Virginia 22042

2a. REPORT SECURITY CLASSIFICATION
UNCLASSIFIED

2b. GROUP

3. REPORT TITLE
RESEARCH AND DEVELOPMENT OF DISCONTINUOUS FIBER REINFORCED LIGHT ALLOYS

4. DESCRIPTIVE NOTES (Type of report and inclusive dates)
Final Report (March 1971 - March 1972)

5. AUTHOR(S) (First name, middle initial, last name)
Robert A. Hermann, Paul J. Lare, Fred Ordway, and Henry Hahn

6. REPORT DATE
May 1972

7a. TOTAL NO. OF PAGES
49

7b. NO. OF REFS
4

8a. CONTRACT OR GRANT NO.
N00017-71-C-4404

b. PROJECT NO.

c.

d.

9a. ORIGINATOR'S REPORT NUMBER(S)
7016-FR

9b. OTHER REPORT NO(S) (Any other numbers that may be assigned this report)

10. DISTRIBUTION STATEMENT
Approved for public release; distribution unlimited.

11. SUPPLEMENTARY NOTES
Details of Illustrations in this document may be better studied on microfiche

12. SPONSORING MILITARY ACTIVITY
DEPARTMENT OF THE NAVY
Naval Ordnance Systems Command
(ORD-0333), Washington, D. C. 20360

13. ABSTRACT

Two approaches to the preparation of titanium alloy composites reinforced with silicon carbide fibers without objectionable fiber-matrix reaction were studied: (1) interposing a protective coating of cerium monosulfide between the fiber and matrix; (2) activated pressure sintering of the metal hydride with the fibers to produce consolidation under less severe conditions. The CeS coating retarded reaction between SiC and pure titanium and remained apparently unaffected up to 930°C for 2 hr, permitting consolidation of the Ti/SiC composite by diffusion bonding. Activated sintering of the hydride at 800°C for 3 hr gave Ti-10V/SiC composites demonstrating improvement in tensile strength and an increase in elastic modulus as predicted by the law of mixtures for the low fiber contents employed. Use of Ti-30V hydride gave a well consolidated product also, but of lower tensile strength.

Composites of 2024 aluminum reinforced with discontinuous graphite fibers (Thornel 75 and Modmor Type 1) were prepared by liquid-phase hot pressing of metal powder-fiber green bodies. Alignment of fibers was obtained by hot extrusion of the consolidated composite or camphene extrusion and layup of the original green body. Hot extrusion produced severe fiber damage and strength inferior to that of the unreinforced matrix. The prealigned, hot pressed specimens also had poor mechanical properties due to inadequate penetration and bonding of the matrix.

| 14. KEY WORDS | LINK A | | LINK B | | LINK C | |
|---|---|---|---|---|---|---|
| | ROLE | WT | ROLE | WT | ROLE | WT |
| Extrusion | | | | | | |
| Fiber Alignment | | | | | | |
| Tensile Properties | | | | | | |
| Whisker Composites | | | | | | |
| Titanium Hydride | | | | | | |
| Titanium Composites | | | | | | |
| Silicon Carbide | | | | | | |
| CeS Barrier Coatings | | | | | | |
| Activated Pressure Sintering | | | | | | |
| Ti-V Alloys | | | | | | |
| Thornel | | | | | | |
| Modmor | | | | | | |
| Graphite fibers | | | | | | |

# RESEARCH AND DEVELOPMENT
# ON
# DISCONTINUOUS FIBER REINFORCED LIGHT ALLOYS

March 1971 - March 1972

FINAL REPORT

By

R. A. Hermann
P. J. Lare
F. Ordway
H. Hahn

Prepared under Contract N00017-71-C-4404

for

DEPARTMENT OF THE NAVY
Naval Ordnance Systems Command (ORD-0333)
Washington, D. C. 20360

by

ARTECH CORP.
2816 Fallfax Drive
Falls Church, Virginia 22042

7016-FR

# ACKNOWLEDGEMENTS

Grateful acknowledgement is made of the continued guidance and helpfulness of Mr. Marlin Kinna and Mr. Sol Matesky, Naval Ordnance Systems Command, during the course of this program. The fabrication and testing reported herein were carried out by Leah Loy, Russell Rowe, Orville VanBlaricon, and John Hefner of ARTECH.

# ABSTRACT

Two approaches to the preparation of titanium alloy composites reinforced with silicon carbide fibers without objectionable fiber-matrix reaction were studied: (1) interposing a protective coating of cerium monosulfide between the fiber and matrix; (2) activated pressure sintering of the metal hydride with the fibers to produce consolidation under less severe conditions. The CeS coating retarded reaction between SiC and pure titanium and remained apparently unaffected up to 930°C for 2 hr, permitting consolidation of the Ti/SiC composite by diffusion bonding. Activated sintering of the hydride at 800°C for 3 hr gave Ti-10V/SiC composites demonstrating improvement in tensile strength and an increase in elastic modulus as predicted by the law of mixtures for the low fiber contents employed. Use of Ti-30V hydride gave a well consolidated product also, but of lower tensile strength.

Composites of 2024 aluminum reinforced with discontinuous graphite fibers (Thornel 75 and Modmor Type 1) were prepared by liquid-phase hot pressing of metal powder-fiber green bodies. Alignment of fibers was obtained by hot extrusion of the consolidated composite or camphene extrusion and layup of the original green body. Hot extrusion produced severe fiber damage and strength inferior to that of the unreinforced matrix. The prealigned, hot pressed specimens also had poor mechanical properties due to inadequate penetration and bonding of the matrix.

# TABLE OF CONTENTS

## LIST OF ILLUSTRATIONS

Figure Page

# LIST OF TABLES

# SECTION 1

## INTRODUCTION

The ultimate objective of this program is to realize in practical service the potential performance of light, high-strength alloys (particularly those of aluminum and titanium) with reinforcement by fibers of extremely high strength such as boron, aluminum oxide, silicon carbide, and graphite. The previous work has emphasized the use of single-crystal whiskers as reinforcement because such fibers represent the highest strengths likely to become available for the purpose. The whisker material on which commercial production efforts have been most concentrated is beta silicon carbide, and the concurrent work at ARTECH has developed techniques for preparing composites of aluminum and magnesium alloys reinforced with SiC whiskers. The SiC whisker composites have been shown to attain strengths almost as high as boron-aluminum continuous filament composites and comparable to fully heat treated high strength titanium alloys, and elastic moduli much higher than the alloys.

Extensive evaluation of these composites is inhibited by the present small supply and high cost of whisker materials, although the work on the commercial production of the whiskers is continuing. High strength graphite fibers, on the other hand, are now available at lower cost and in ample supply for research and development purposes. A part of the work covered by this report was therefore devoted to developing aluminum alloy composites reinforced with discontinuous graphite fibers. The composite preparation techniques developed for whisker reinforcement were applicable to the composites reinforced with chopped graphite filaments, and the advantages of discontinuous fiber reinforcement (possibility of hot working or forming, better off-axis strength) should also obtain for the graphite composites.

The light alloys with highest strength, and also with highest elevated temperature structural performance, are those of titanium. The application of the previously developed whisker composite fabrication techniques to titanium matrix composites is frustrated by the reactivity of the matrix with SiC, which prohibitively degrades the SiC whiskers at the temperature required for composite consolidation. The effective study of consolidation and reactivity requires that the reaction layer be considerably smaller than the radius of the fiber. Thus the system may be studied, and possibly also used in practice, with large diameter fibers when the reaction rate is so high that the fine whiskers are degraded completely. Accordingly, the substitution of the commercially available 0.004-in. (100-μm) SiC filaments for the whiskers of diameter 0.1-3 μm suggests itself.

The use of a cerium monosulfide coating to inhibit fiber-matrix reaction was suggested because of the high thermodynamic stability of CeS, and was initially tested with the 0.004-in. SiC filaments diffusion bonded in a pure titanium matrix. The results are sufficiently encouraging to justify further study.

Another approach to the reduction of fiber degradation during consolidation of a Ti/SiC composite is the use of titanium hydride rather than the pure metal. The decomposition of the hydride during sintering increases atomic mobility and permits such activated pressure sintering to be carried out under less severe conditions of temperature and pressure, with corresponding reduction in the rate of the fiber-matrix reaction.

The degradation of SiC fibers is known to be less rapid in titanium vanadium alloys than in pure titanium. To obtain a well consolidated composite with the least initial fiber-matrix reaction and also the best stability in elevated-temperature service, the study of activated pressure sintering of Ti-10V and Ti-30V hydrides, as well as that of Ti, reinforced with SiC filaments, was planned.

# SECTION 2

# EXPERIMENTAL PROCEDURES

## 2.1 Materials

### 2.1.1 Metal Matrices

The matrices used in this program were titanium alloys and aluminum alloys. Commercially pure titanium sheet stock 0.032 in. thick was utilized in the evaluation of the CeS coated SiC fibers. Titanium-vanadium hydride powder, -400 mesh, containing ten and thirty weight percent vanadium was produced by Oremet Corp., Albany, Oregon. The Al-2.5Si matrix was a mixture of 75% pure aluminum powder with 25% LS-789 Al alloy powder obtained from the Reynolds Metal Company, Richmond, Virginia. The particle size of the pure aluminum powder was 6-10 μm and that of the LS-789 was less than 37 μm. The 2024 Al atomized powder, obtained from the Reynolds Metals Company, Richmond, Virginia, was sieved and +100 mesh and -400 mesh fractions were utilized for the composite matrices.

### 2.1.2 Reinforcing Fibers

Silicon carbide fibers of 0.004-in. diameter, obtained from Thompson CSF, Orlay, France, were used as substrate for the CeS coating experiments and as the reinforcement in the Ti-V matrix composite. Two types of graphite fibers were used as reinforcement in the Al alloy composites; Modmor Type 1 chopped to 1/4-in. average length, obtained from Fothergill & Harvey Limited, Littleborough, Lancs., England, and Thornel 75 (grade WYL 160-1/2) chopped to an average length of 1/2 in., obtained from the Union Carbide Corporation, Greenville, South Carolina.

## 2.2 Composite Preparation and Consolidation

### 2.2.1 Titanium Test Pieces Reinforced with CeS-Coated SiC

Test samples for determination of the thermal stability of CeS in titanium were prepared by coating 1/4 x 1/4 x 0.032 in. titanium sheet stock, polished with six-micron diamond powder, with cerium monosulfide by rf sputtering as described in previous reports.(1)

In the first experiment, three CeS-coated titanium samples were heated for two hours in a vacuum of 5 x $10^{-6}$ torr at 800, 900, and 1,000°C respectively. The coating thickness was found to be unmeasurable on all three specimens after treatment, possibly because the stable CeS was degraded by reaction with residual oxygen. A second experiment was carried out in which coated samples were bonded to uncoated titanium plates at various temperatures. Test samples were prepared as follows:

(1) Polish 1/4-in. squares of Ti sheet stock.

(2) Vacuum anneal samples at 1000°C for 5 min.

(3) RF sputter half the squares with CeS as previously described.(1)

(4) Place larger Ti discs over top and bottom of paired squares with CeS coating between them.

(5) Diffusion bond samples in vacuum at a pressure of 6000 psi and temperatures of 800°, 900°, and 1000°C respectively for 2 hr.

Samples were prepared for metallography by potting in alumina-filled epoxy and sectioning normal to the coating.

In order to study reaction of Ti with SiC filaments, specimens were diffusion bonded under the same conditions as for previously prepared coated filament samples(1); 1500°, 1600°, and 1700°F and 600 psi for 2 hr. Transverse sections were prepared for metallography and scanning electron microscopy as described in section 3.

To study the fracture of Ti/CeS/SiC composites in transverse tension, a specimen was prepared with a single layer of coated fibers aligned transversely. For this purpose, tensile specimens having an overall length of 1-13/32 in. and 1/2-in. width, with a reduced section 1/2 in. long and 1/4 in. wide, were machined from 1/32-in. titanium sheet. Transverse grooves 0.006 in. square were machined across the reduced section on 1/32-in. centers. In preparing the first specimens a CeS-coated SiC fiber was cemented in each groove with purified camphene. An ungrooved tensile specimen was placed on top and the assembly was carefully positioned in a zirconia hot-press die. After evaporation of the camphene, the composite was vacuum hot pressed at 1500°F for 1 hr at 6,000 psi. A specimen without fibers was consolidated in an identical manner. Both specimens were ground flat on both sides, remachined to the original profile, and tested in tension.

Additional composite samples, having three layers of filaments, were prepared for testing by the same procedure.

### 2.2.2 SiC-Reinforced Ti-V Prepared by Activated Pressure Sintering

A series of 16 unreinforced samples of 0.690-in. diameter was consolidated from Ti-V hydride powder by vacuum hot pressing, and in some cases by an additional sintering cycle, to determine the consolidation parameters. The processing parameters and densities of the samples are given in Table I.

TABLE I

PROCESSING PARAMETERS AND DENSITIES FOR SAMPLES CONSOLIDATED FROM TITANIUM-VANADIUM HYDRIDE POWDERS

| | | Consolidation Conditions | | | Sintering | | |
|---|---|---|---|---|---|---|---|
| Sample | Composition | Pressure psi | Temp. °C | Time hr | Temp. °C | Time hr | Density |
| 3 | Ti-10V | 4000 | 600 | 1 | 800 | 1 | * |
| 4 | Ti-30V | " | 600 | 1 | 800 | 1 | * |
| 5 | Ti-10V | " | 600 | 1 | --- | - | * |
| 6 | Ti-30V | " | 600 | 1 | --- | - | * |
| 7 | Ti-10V | " | 600 | 3 | --- | - | * |
| 8 | Ti-30V | " | 600 | 3 | --- | - | * |
| 9 | Ti-10V | " | 700 | 1 | --- | - | * |
| 10 | Ti-30V | " | 700 | 1 | --- | - | * |
| 11 | Ti-10V | " | 700 | 3 | --- | - | 3.82 |
| 12 | Ti-30V | " | 700 | 3 | --- | - | 4.16 |
| 13 | Ti-10V | " | 800 | 1 | --- | - | 4.39 |
| 14 | Ti-30V | " | 800 | 1 | --- | - | 4.50 |
| 15 | Ti-10V | " | 800 | 3 | --- | - | 4.53 |
| 16 | Ti-30V | " | 800 | 3 | --- | - | 4.77 |

---

*Readings drifted when weighed in alcohol, indicating porosity.

The lower limit of consolidation temperature was established in previous work as 800°C for 1 hr for hydrided Ti-10V and Ti-30V alloys without reinforcement. Compatibility samples, containing SiC fibers set in the loose hydride alloy powders in the die, were therefore consolidated at that temperature for evaluation. Additional samples were consolidated at 800°C for 3 hr when longer pressing was found to be warranted by the limited reaction observed in the 1-hr samples.

Small laid-up samples to study the feasibility of this technique were prepared from the hydride powder and the SiC fibers by mounting the fibers in a grooved frame, melting camphene around them to facilitate handling, and sandwiching the fiber layer between strips of camphene-powder mixture in a suitable die. Most of the camphene was then removed by melting from the bottom while a small force was applied to the top of the stack by a plunger.

The first such composite specimen, pressed primarily to assess the layup technique as well as the consolidation, was vacuum hot pressed at 800°C for 2 hr. A second specimen was prepared using a slurry of powder and camphene around the fibers, instead of camphene alone, in order to pin the fibers during the camphene removal, and pressed for 3 hr. While both specimens (Ti10V-34 and Ti10V-35) were well consolidated, the matrix powder in the camphene slurry caused an uneven distribution of the fibers in specimen 35.

Four composite samples were prepared by this camphene coating technique, the two prepared from Ti-10V and two prepared from Ti-30V hydride powder in the same manner as specimen 34 but with 3-hr pressing.

### 2.2.3 Carbon Filament Reinforced Al Alloy Composites

#### 2.2.3.1 Camphene Aligned, Liquid Phase Hot Pressed Composites

The technique first used to prepare camphene infiltrated green bodies for consolidation was similar to that previously developed for whisker reinforced composites. Namely, a green strength powder-fiber cake was prepared by filtering an isopropyl alcohol suspension of Al alloy powder and chopped C fibers, and subsequently the dried cake was infiltrated with liquid camphene and frozen to 0°C. This technique proved unsatisfactory because the green body contained stratified layers, and undispersed bundles of fibers were observed in the composites.

Several other techniques, such as infiltrating loosely packed fiber mats with coarse powder, chips, and fine (-400 mesh) powder dispersed in liquid camphene, were attempted and proved unsatisfactory. It was considered possible that surface impurities were present which inhibited contact and wetting of the fibers by the metal during final consolidation.

To eliminate any effects of such impurities, the Thornel fibers were washed three times in boiling water and fired in nitrogen at 900°F to remove any polyvinyl alcohol sizing. The previous technique was used for the preparation of green bodies, but the treated fibers were coated with nickel to improve the penetration of the liquid matrix and eliminate porosity. An initial composite prepared in this way was significantly improved, but the preparation of several additional composite specimens exposed new problem areas. The process of coating the fibers, using the thermal decomposition of $Ni(CO)_4$, proved to be slow and nonuniform. The thickness of the fiber mat that could be coated was limited by the tendency for the exterior of the mat to be excessively coated while the interior was coated insufficiently.

The composite specimens made with the nickel-coated fibers also had the stratified structure that had been observed in the previous specimens. To eliminate this stratification, the technique of preparing green bodies was restudied. Suspensions of matrix powder and graphite fibers in isopropyl alcohol and in acetone were made and their settling rates were observed. The sediment was found generally to be a mixture of powder and fibers significantly more uniform than had been obtained by the previous technique. When the liquid was rapidly removed, however, it carried the matrix powder through the mat structure formed by the fibers. Melted camphene was tried as the suspending liquid because it must be added eventually in any case to form the extrudible billet for fiber alignment. In a glass tube of proper size for the billet, with a removable Teflon plug, an ultrasonically agitated mixture of melted camphene, matrix powder, and graphite fibers in correct proportion for a 40 v/o composite was held in an oven at a temperature slightly above the melting point of the camphene, and the mixture was allowed to settle without any additional stirring. After sedimentation had been completed, the container was carefully removed from the oven to permit solidification of the camphene. Voids were not created in the resulting billet because solidification progressed slowly and the sediment occupied less than one third of the container's height.

The tube was warmed with a hot air blower and the billet was extruded with a plunger. The portion containing the matrix-fiber mixture was sliced along its longitudinal axis and examined for uniformity. As in the earlier sedimentation experiments with other liquids, the -400 mesh matrix powder and the graphite fibers appeared to have similar settling rates in the melted camphene, and to produce a homogeneous mixture superior to that given by previous methods of forming the billets.

The two halves of the billet were then reapposed and extruded into bars of 1/8-inch square cross section. The uniformity of dispersion was preserved during the extrusion to align the graphite fibers. Additional billets were prepared in the same manner and extruded to provide material for fabricating a composite specimen. The first such composite, containing 40 v/o fibers, was of superior quality. Metallographic examination indicated that the problems of stratification and porosity were essentially eliminated by the changes in technique.

On the basis of these results, composite specimens were fabricated in the same way for determination of the mechanical properties as a function of the fiber content. The processing parameters and densities for these composites of 2024 Al containing 20, 30, and 40 v/o filaments (samples 27-38 inclusive) are listed in Table II together with those of all the previous samples.

### 2.2.3.2 Hot Extruded 2024 Al/C Composites

Two extrusion billets were prepared by liquid phase hot pressing metal powder-fiber filter cakes at 600°C and 3,000 psi and subsequently stacking three pressed sections in an 1100 Al can of 0.025-in. wall thickness and pressure bonding the pieces together at a temperature slightly above the solidus. The experimental conditions and billet densities are listed in Table II (pressings C-2 through C-7 inclusive). The billets, 1-1/8 in. in diameter and 1-1/2 in. long, were hot extruded at a rate of 0.1 in./min. and a temperature of 480°C to a final diameter of 5/16 in. and lengths of 11.5 in. and 14 in. respectively.

# TABLE II

## PROCESSING PARAMETERS AND DENSITIES FOR ALUMINUM ALLOY/DISCONTINUOUS CARBON FIBER COMPOSITES

| Sample | Fiber Content v/o | Matrix | Pressure psi | Temperature °C | Alignment Procedure | Density g/cm$^3$ | Comment |
|---|---|---|---|---|---|---|---|
| C-1 | 20 | Al-2.5 Si | 3000 | 585 | Camphene Extruded | 2.55 | |
| C-2 | 20 | 2024 Al | 3000 | 600 | Hot Extruded at 480°C and 0.1 in/min. | 2.59 | First extrusion; billet density 2.59 g/cm$^3$. |
| C-3 | " | " | " | " | " | 2.57 | |
| C-4 | " | " | " | " | " | 2.59 | |
| C-5 | 20 | 2024 Al | 3000 | 600 | " | 2.59 | Second extrusion; billet density 2.61 g/cm$^3$. |
| C-6 | " | " | " | " | " | 2.59 | |
| C-7 | " | " | " | " | " | 2.60 | |
| C-8 | 20 | 2024 Al | 3000 | 600 | Camphene Extruded | 2.59 | 2024 Al chips used. Loose fiber mat infiltrated with -400 mesh 2024 Al. |
| C-9 | " | " | " | " | " | 2.57 | |
| C-10 | " | " | " | " | " | 2.59 | |
| C-12 | 40 | " | 3000 | 615 | " | 2.42 | " Applied pressure at 600°C on cooling. |
| C-13 | 0 | " | 3000 | 615 | n/a | 2.79 | Made to check press monitoring system, die, and parameters. |
| C-14 | 0 | " | " | 600 | " | -- | |
| C-15 | 0 | " | " | 600 | " | -- | |
| C-16 | 0 | " | " | " | " | 2.62 | |
| C-17 | 0 | " | " | " | " | 2.69 | |
| C-18 | 40 | Al-12.5Si | 3000 | 575 | Camphene Extruded | 2.62 | Made with this alloy for improved wetting, did not penetrate fiber bundles |

## Table II (Continued)

| | | | | | | | |
|---|---|---|---|---|---|---|---|
| C-19 | 40 | 2024 Al | 3000 | 575 | Camphene Extruded | 2.52 | Thornel fibers Ni coated, pressed at wrong temp. |
| C-20 | " | " | " | 600 | " | 2.57 | Thornel fibers, CVD Ni coated. |
| C-21 | " | " | " | 600 | " | | Thornel fibers. |
| C-22 | " | " | " | " | " | | Replacement for C-20. |
| C-23 | " | " | " | 610 | " | 2.36 | Modmor fibers, prepared by sedimentation technique |
| C-24 | " | " | " | 610 | " | 2.30 | Thornel fibers, |
| C-25 | " | " | " | 610 | " | --- | Thornel fibers, trouble during pressing. |
| C-26 | " | " | " | 600 | " | 2.35 | Thornel fibers. (1) |
| C-27 | " | " | " | " | " | 2.33 | " |
| C-28 | " | " | " | " | " | 2.32 | " |
| C-29 | 30 | " | " | 600 | " | 2.46 | " |
| C-30 | " | " | " | " | " | 2.44 | " (1) |
| C-31 | " | " | " | " | " | 2.43 | " |
| C-32 | 20 | " | " | " | " | 2.53 | " (1) |
| C-33 | " | " | " | " | " | 2.57 | " |
| C-34 | " | " | " | " | " | 2.57 | " |
| C-36 | 40 | " | " | " | Camphene Extruded Transverse | 2.33 | " (1) |
| C-36 | 30 | " | " | " | " | 2.43 | " (1) |
| C-37 | 20 | " | " | " | " | 2.53 | " (1) |
| C-38 | 40 | " | " | " | Camphene Extruded Longitudinal | | Modmor fibers. |

---

(1) Heat treated--T6--solution at 910° for 5 hr, water quench, age at 365°F for 8 hr.

# SECTION 3

# TESTING PROCEDURES

## 3.1 Mechanical Testing

Tensile testing was performed on an Instron machine, floor model TTC. A chart speed of 2 in./min was employed. A strain rate of 0.02 in./in./min was used in the majority of cases. The elastic modulus was determined by use of a 10%, 1/2-in. strain gage extensometer in conjunction with an X-Y chart recorder. The strain was read directly from the recorder chart and the stress computed from the load values.

## 3.2 Metallography

Standard mounting and polishing techniques were used to prepare composite specimens for metallographic examination. A hard mounting medium, Buehler No. 20-8130AB epoxide compound (oven-cured), was preferred in order to reduce rounding of the specimen edges.

Grinding with Varsol on SiC papers through 600 grit was used to prepare the specimens for the polishing operation. Polishing with diamond abrasives of -15, -6, -3, and -1 micron grit sizes was found to be most effective regardless of the fiber content of the specimen. Polishing papers, giving a comparatively hard lap surface, were most effective in minimizing relief at the fiber-matrix interfaces. With the titanium composite specimens, polishing was done with chromic acid-levigated alumina slurries on low nap cotton cloth. Final polishing was done using chromic acid-levigated 0.05 micron alumina on Microcloth.

Standard etchants for aluminum and titanium alloys were used to outline the fibers, bring out the grain boundaries, and remove disturbed metal at fiber-matrix interfaces.

## 3.3 Density

The specimens were ultrasonically cleaned in a series of reagent grade solvents prior to determining the density. The first solvent, benzene, was followed by acetone, then deionized water, and finally ethanol, followed by oven drying. Several specimens, prior to cleaning, required fine grinding to remove graphite adhering to the surface.

The displacement method was used to determine the densities of all specimens. Isopropyl alcohol was used as the immersion liquid because its low surface tension permitted penetration of surface porosity, which could be detected by the displacement of air bubbles or by a slow increase in weight.

## 3.4 Electron Microscopy

Samples for electron microscopy were prepared by single and two-stage replica techniques. Single stage replicas were prepared using 1% collodion solutions. The replica film was shadowed with chromium at an angle of approximately 30° and stabilized with carbon. Two stage replicas were prepared by softening cellulose acetate film in acetone and pressing the film on the sample surface. When dried, the cellulose acetate film was removed and shadowed as above. The plastic film was dissolved by extraction in an acetone reflux apparatus.

# SECTION 4

# RESULTS AND DISCUSSIONS

## 4.1 CeS Coating as a Protection for SiC in Ti

The relative stability of various refractory sulfides has been reviewed by Litz and Blocher(2). Aluminum, calcium, and magnesium have been shown to reduce all titanium sulfides to the metal. The free energy curve for CeS is roughly parallel to and substantially below the curves for the sulfides of all these metals. The relative instability of CaS increases from 10 kcal/mole at room temperature to about 30 kcal/mole at 1700°C. The free energy of MgS is higher than that of CeS by about 75 kcal/mole at room temperature, increasing to about 115 kcal/mole at 1700°C. Aluminum sulfide is less stable than CeS by about 130 kcal/mole. The free energy of titanium sulfide being still higher, the corresponding ratio of chemical activities at 1,000°C, for example, is more than $10^{20}$. That is, the activity of sulfur in a sample of titanium in equilibrium with the CeS and Ce phases would be $10^{-20}$ times the activity of sulfur in the titanium sulfide. If the atomic ratio were directly proportional to the activity, then the titanium phase would contain only one atom of sulfur for every $10^{20}$ atoms of metal. Even if this estimate is in error by many orders of magnitude, the sulfur content in titanium equilibrated with CeS must be undetectably small.

In the previous year's work on this program(1), SiC-CeS-Ti compatibility samples, prepared by diffusion bonding CeS-coated SiC fibers between Ti sheets at 816°C for 2 hr, had been found on metallographic examination of cross sections and taper sections to show some evidence of reaction zones. This question was further studied by compatibility tests of CeS-Ti samples and scanning electron microscopy of the SiC-CeS-Ti samples previously prepared. In addition, comparison samples were made similarly from uncoated SiC fibers in Ti.

In the first attempted compatibility tests, CeS-coated Ti samples prepared as described in section 2.2.1 were heated in vacuum at 800, 900, and 1000°C. Visual examination of the samples after heating revealed a color change. The 800° sample remained steel-blue, while the 900°C sample became straw colored and the 1,000°C sample a light yellow. Metallographic examination of the samples showed no evidence of a reaction zone in the titanium, but no measurable coating thickness. It is hypothesized that oxidation of the coating permitted its reaction with the titanium and diffusion of some nonvolatile reaction products into the bulk metal.

A second experiment was performed to determine the reaction rate and bonding characteristics of the Ti-CeS interface with the atmosphere excluded. In this experiment, 1/4-in. square coated samples were diffusion bonded at temperatures of 800°, 900°, and 1000°C as described in section 2.2.1 and subsequently examined for evidence of bonding and reaction at the interfaces between the coating and the two titanium sheets. Representative photomicrographs of the CeS-Ti interfaces in these samples are shown in figure 1. Although no diffusion zone is visible, the coating thickness appears reduced as the consolidation temperature increases. This observation would show, in the absence of other information, comparatively rapid degradation of the CeS coating in contact with Ti.

The reaction between uncoated SiC and Ti was observed by preparing diffusion bonded samples under the same conditions as with the coated filament samples: 1500°, 1600°, or 1700°F and 6000 psi for 2 hr. Cross sections of the uncoated SiC-Ti samples shown in figure 2 show a definite reaction zone, which increases in width with increasing consolidation temperature.

Metallographic examination of the CeS coated samples had indicated that the coating maintained its integrity. To investigate the possible presence of a reaction zone, the samples were subjected to scanning electron microscopy.

Figure 3(a) is a scanning electron micrograph of the cross section of the sample pressed at 1700°F for 2 hr showing the fiber-coated-matrix region. The bright areas seen at the outer edge of the fiber and the outer edge of coating are differences in reflectivity caused by rounding of the respective edges and differences in height produced by etching. Also seen in figure 3 (b, c, d) are X-ray maps representing Ti, Ce, and Si in the sample, obtained by setting the discriminator of the nondispersive X-ray detector in the scanning electron microscope for the corresponding pulse amplitude. In each case, the element is concentrated in the region where it is known to be a major constituent, with a lower "background" indication elsewhere. The maps appear to reveal no interdiffusion, which would blur the sharp interfaces. The Ce map in figure 3(c) shows a more intense, but uniform, background in the Ti region than in the SiC region. This difference is believed to arise from differences in excitation characteristics of the two materials, however, rather than Ce content. The narrow ring in the Ti map, figure 3(b), is almost certainly due to the effect of the high rounded edge of the SiC on the instrumental response rather than to any Ti concentration between the SiC and CeS.

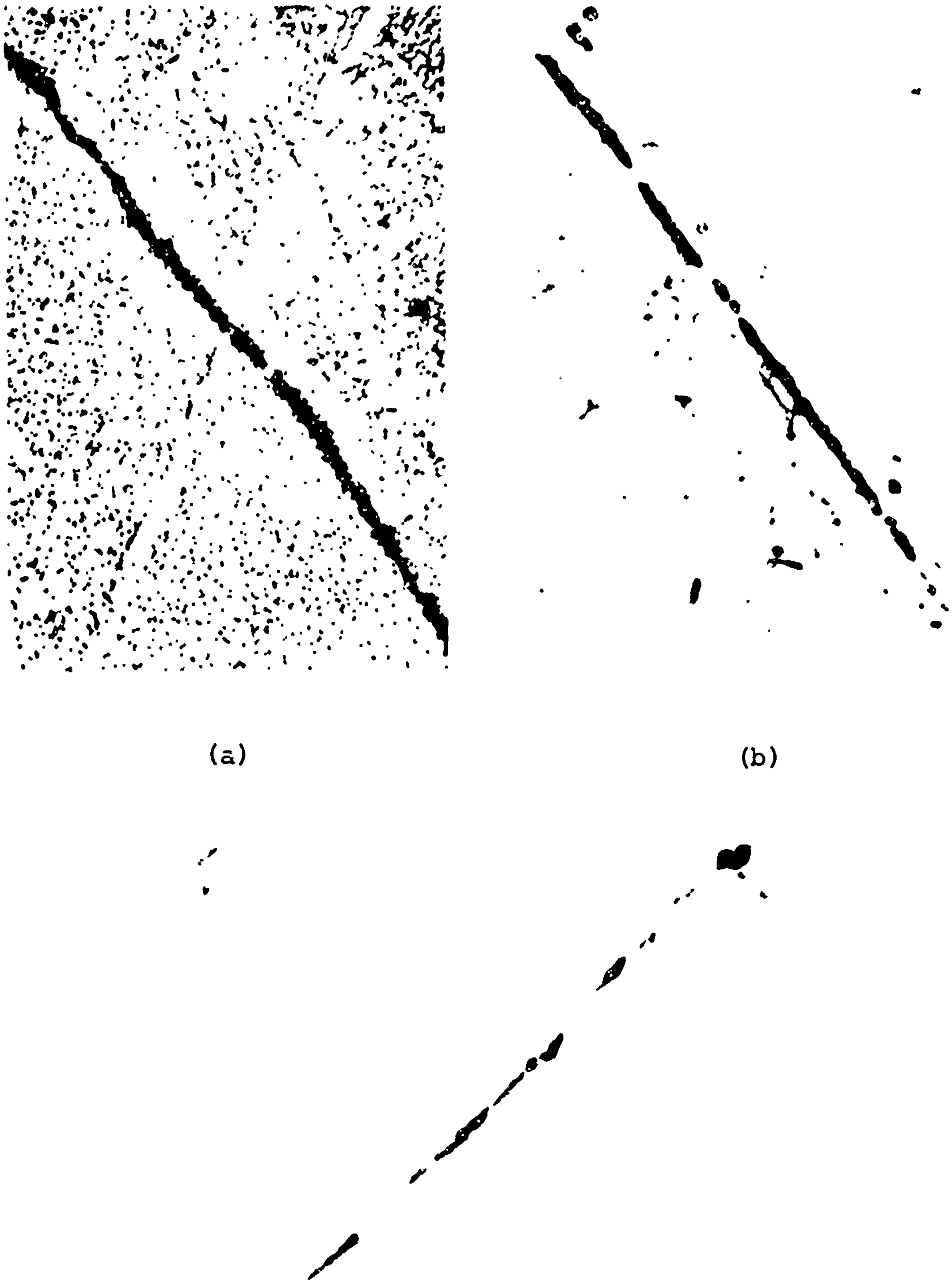

(a)

(b)

(c)

Figure 1. Interfaces between sputtered CeS coating and titanium in samples pressed at (a) 800°C, (b) 900°C, and (c) 1000°C (X1500).

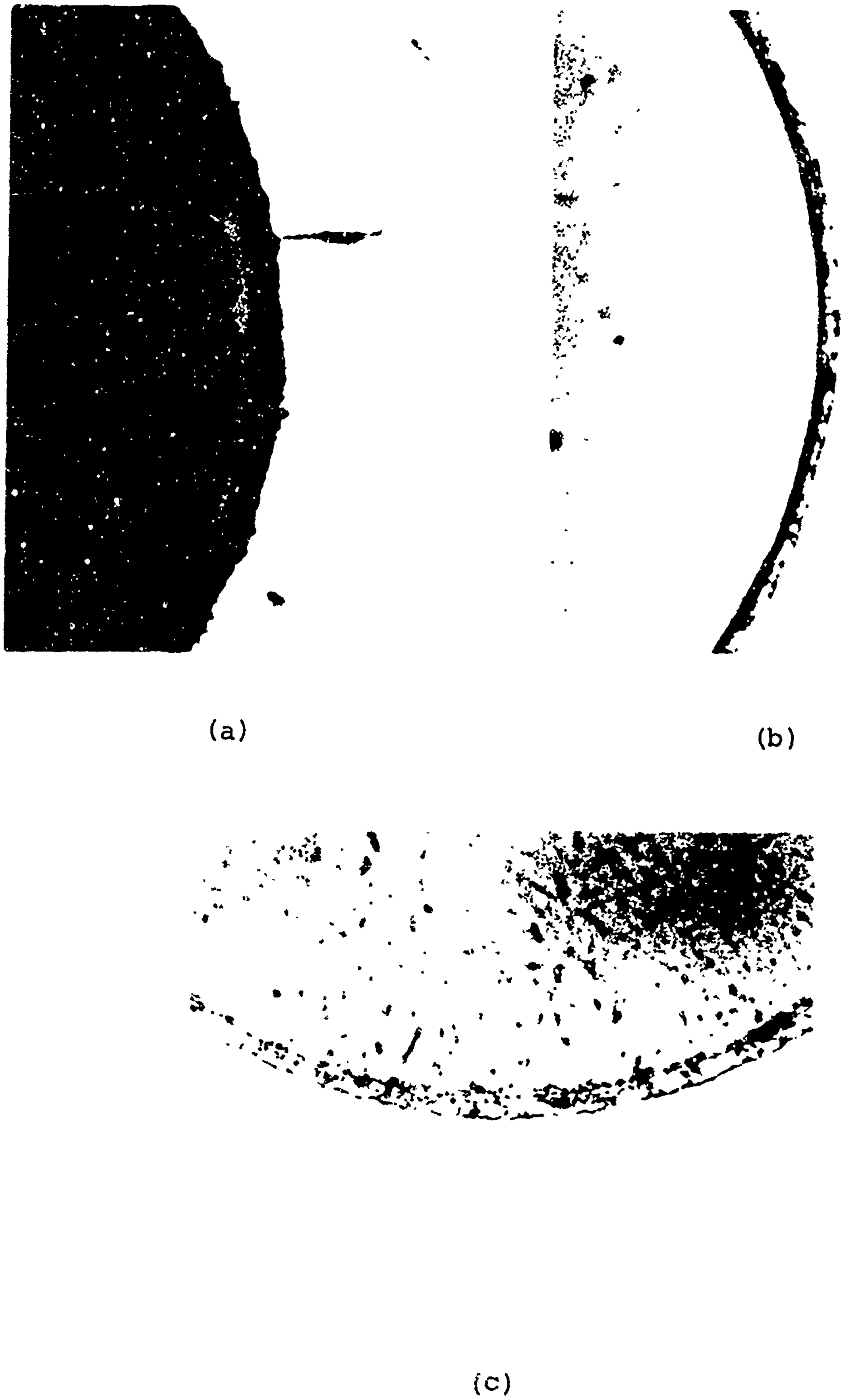

Figure 2. Interface between SiC filament and titanium consolidated for 2 hr at (a) 1500°F, (b) 1600°F, and (c) 1700°F (X1500).

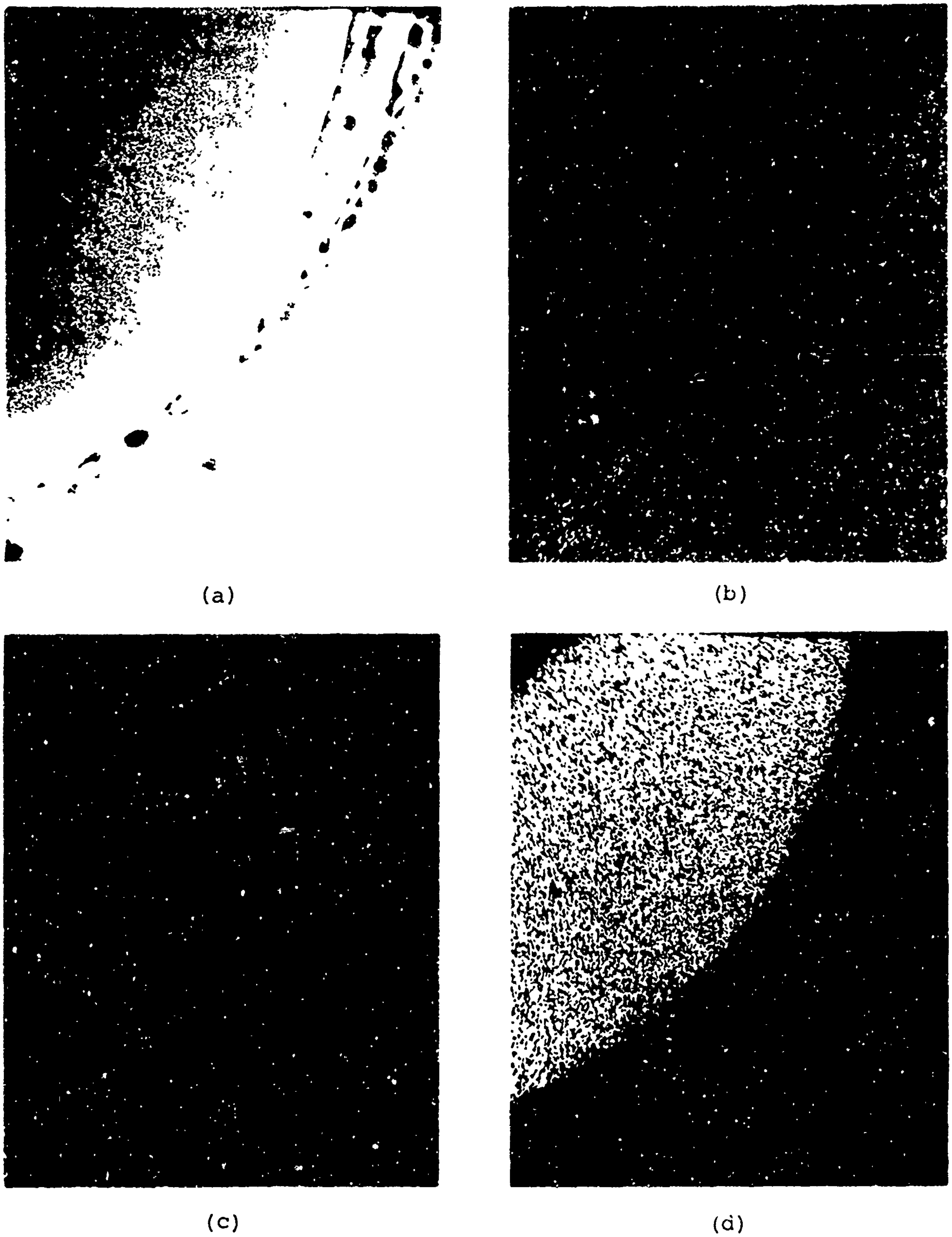

(a) (b)

(c) (d)

Figure 3. Ti CeS coating SiC filament interfaces (X2200) in sample consolidated at 1700°F for 2 hr: (a) scanning electron micrograph, (b) Ti X-ray map, (c) Ce X-ray map, and (d) Si X-ray map.

These results left in question whether detectable reaction had occurred in the SiC-CeS-Ti samples, but clearly showed that the coating greatly reduces the rate of interaction between SiC and Ti. As the strength of the bond of the coating to the fiber and to the matrix was in question, it was decided to prepare a specimen with a single layer of coated fibers arranged transversely so that the path of the fracture could be identified as passing either through a fiber or along the interface. Additional composite samples having three transverse layers of filaments were also tested.

The tensile strength of the matrix and of the single layer transverse samples were essentially the same, 100 kpsi. The three-layer sample had a strength of approximately 85 kpsi. Examination of the fracture surfaces in the composite samples indicated that failure occurred along the interface between the CeS coating and the SiC fibers. The circumstances under which failure would occur at the fiber surface was considered in terms of a simple two-phase physical model, consisting of a high-modulus fiber in a low-modulus matrix.

The elastic stresses in such an aligned composite under transverse tension may be considered as plane stresses around a cylindrical inclusion of infinite length whose axis is normal to the plane. When the fiber concentration is comparatively low, the situation is approximated by the case of an isolated inclusion. In this case, the maximum normal tension across the fiber-matrix interface occurs on the diameter parallel to the tensile stress $[\sigma_m]_{r=\infty}$ in the matrix far from the inclusion. The magnitude of the interfacial tension$^{(3)}$ is larger than $[\sigma_m]_{r=\infty}$ by a factor $1+(K_1+K_2)/2$ where

$$K_1 = \frac{E_f\ (1-\mu_m) - E_m\ (1-\mu_f)}{E_f\ (1+\mu_m) + E_m\ (1-\mu_f)}\ ,$$

$$K_2 = \frac{E_f\ (1+\mu_m) - E_m\ (1-\mu_f)}{E_f\ (3-\mu_m) + E_m\ (1+\mu_f)}\ ,$$

and E and $\mu$ are Young's modulus and Poisson's ratio respectively, with subscript f for the fiber and m for the matrix.

The stress amplification may be estimated, using the numerical values $E_f$ = 70 Mpsi, $E_m$ = 17 Mpsi,

$$K_1 = \frac{70\ (0.7) - 17\ (0.7)}{70\ (1.3) + 17\ (0.7)} = \frac{37.1}{102.9} = 0.360$$

$$K_2 = \frac{70\ (1.3) - 17\ (0.7)}{70\ (2.7) + 17\ (1.3)} = \frac{79.1}{211.1} = 0.375$$

giving

$$1 + \frac{K_1 + K_2}{2} = 1.37.$$

Thus the transverse tension at the most highly stressed location on the fiber-matrix interface is much higher than the average over the whole specimen, which is the value indicated by the testing machine. Tensile yielding would be expected at the interface considerably in advance of yielding elsewhere in the homogeneous matrix. Therefore, it might be expected that the final fracture surface would tend to follow the fiber-matrix interface, as was observed.

The ultimate strength in transverse tensile would not necessarily be so markedly affected by the concentration of elastic stress at the interface, however, as the effect would be mitigated by plastic deformation if the matrix is ductile. Then the strength might simply decrease in proportion to the percentage of fibers (i.e., after yielding, the percentage of voids) in the structure. Such a decrease was qualitatively detected, but the paucity of data makes detailed quantitative interpretation pointless. The important fact established by the experiments was the absence of fiber splitting under transverse tension. The behavior of the interface under shear stresses must be studied by tensile testing of specimens with longitudinal fiber alignment.

### 4.2 Ti-V/SiC Composites Prepared by Activated Pressure Sintering

Activated pressure sintering of Ti-V hydride powder with SiC fibers was investigated as a possible means of consolidating and bonding the composite at sufficiently low temperatures and pressures to avoid fiber damage and degradation. To determine the processing parameters, a series of Ti-V samples without fibers was consolidated as described in section 2.2.2 and evaluated in terms of density and structure. The highest densities and the least porous structure, shown in figure 4, were obtained in samples consolidated at 800°C and 4000 psi for 3 hr.

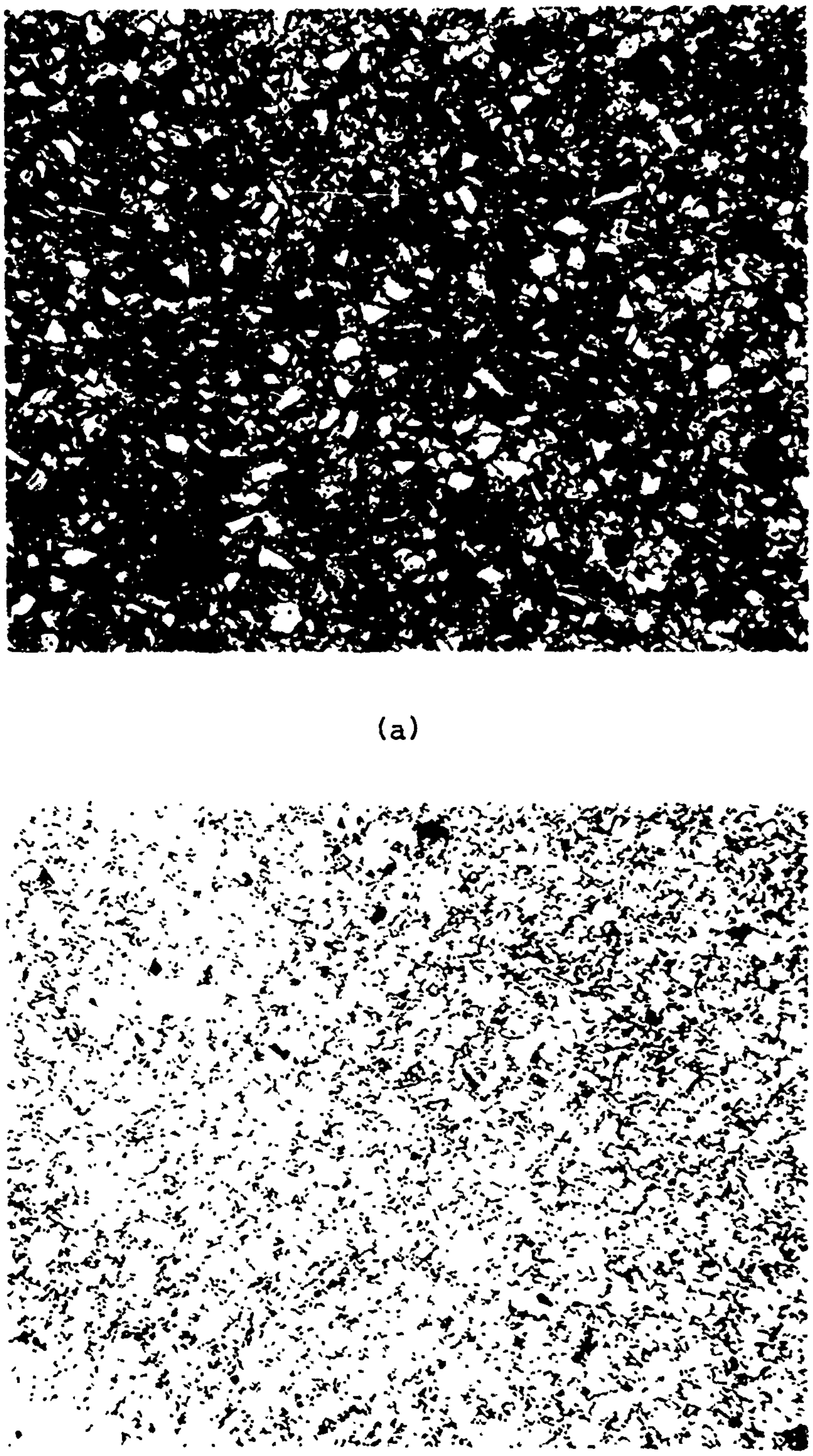
(a)

(b)

Figure 4. Ti-V samples consolidated at 800°C, 4000 psi for 3 hr: (a) 10% V, (b) 30% V (X100).

Based upon the parameters established by the preparation of these unreinforced matrix samples, compatibility samples and samples to assess composite layup techniques were prepared as previously discussed in section 2.2.2. As indicated in figure 5(a), the reaction zone produced in the first compatibility sample by consolidation of the Ti-10V matrix at 800°C for 1 hr appeared sufficiently limited to warrant extending the consolidation time to 3 hr for both matrices. The results are shown in figures 5(b) and 5(c). Electron micrographs of a shadowed replica of the 3-hr Ti-10V sample, shown in figure 6, suggest that the reaction zone in the matrix, although indistinct, is approximately 0.5-1μm wide. This is so narrow as not to affect seriously the properties of the composite. In the case of the Ti-30V matrix there was even less evidence of a reaction zone, indicating even less effect on composite strength. The region over the edge of the fiber, as shown in figure 6, has a lighter appearance which might be taken as evidence of a reaction product in the fiber, but is believed to be merely a difference in shadow density caused by rounding of the fiber edge during polishing.

The results of the mechanical testing performed on the Ti-V samples, with and without SiC fiber reinforcement, are presented in Table III. The unreinforced Ti-30V material has an ultimate tensile strength of approximately 155 kpsi, a yield strength of approximately 140 kpsi, and an elastic modulus of 14 Mpsi as compared to 130 kpsi, 110 kpsi, and 17 Mpsi respectively for the alloy reinforced with approximately 5 v/o continuous SiC filaments. The fibers at the fracture faces of the reinforced samples appear to be broken at the surface rather than pulled out. Some reinforcement is indicated by the the modulus of the composite, but no benefit is noted in the tensile strength. The total strain to fracture in the composite sample is twice that in the unreinforced Ti-30V matrix, however. It is possible that the unreinforced material had abnormally high strength and low ductility because its hydrogen content was not completely eliminated in the consolidation process, the unreinforced sample being significantly thicker than the composite sample.

In the case of the Ti-10V alloy matrix, the comparison of properties shows the 5-6 v/o composite to be about 20 kpsi improved in yield strength, 10 kpsi in ultimate tensile strength, and 5 Mpsi in elastic modulus. The total strain to fracture is about half the matrix value for the composite. These results on the Ti-10V system indicate promise and suggest further work should be performed.

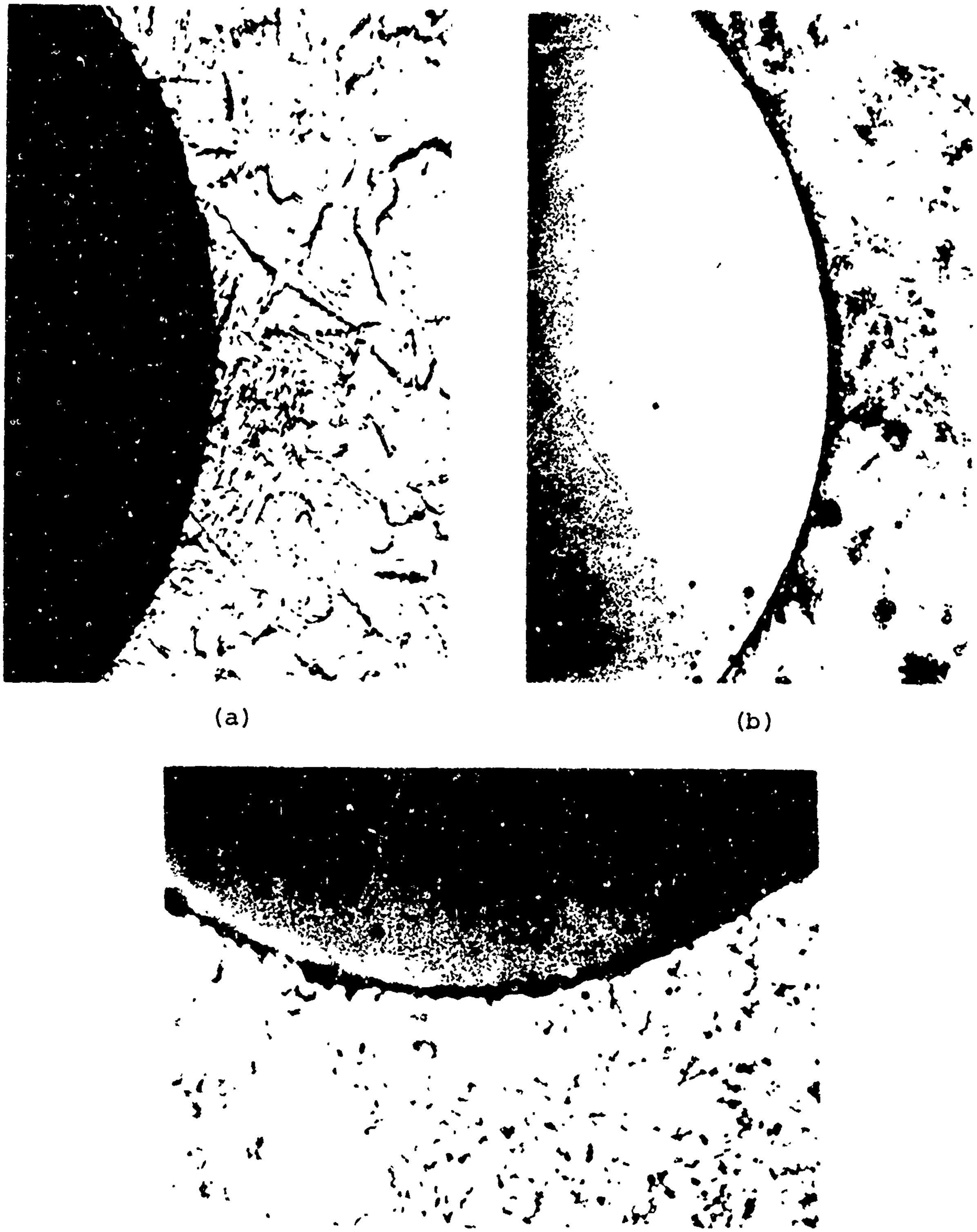

(a)

(b)

(c)

Figure 5. SiC fiber-titanium alloy matrix reaction at 800°C after (a) 1 hr for Ti-10V, (b) 3 hr for Ti-10V, and (c) 3 hr for Ti-30V (X1500).

Ti-10V Matrix SiC Fiber

Figure 6. Replica of SiC fiber/Ti-10V matrix interface after consolidation at 800°C for 3 hr (X10,000).

## TABLE III

## MECHANICAL PROPERTIES OF Ti-V MATRIX COMPOSITES

| | | | Tensile Properties | | | |
|---|---|---|---|---|---|---|
| Test Sample No. | SiC Fiber Content v/o | Cross-Sectional Area in.$^2$ | Yield Strength @0.2% kpsi | Ultimate Strength kpsi | Elastic Modulus Mpsi | Total Strain to Failure in./in. |
| Ti30V-32-1 | --- | 0.01113 | 146.5 | 162.6 | 14.4 | 0.0172 |
| -2 | --- | 0.01107 | 143.6 | 161.7 | 13.7 | 0.0179 |
| -3 | --- | 0.01104 | 139.5 | 154.0 | 14.1 | 0.0155 |
| Ti30V-36 | 5.4 | 0.00794 | 115.9 | 136.0 | 16.8 | 0.0450 |
| Ti30V-37 | 5.5 | 0.00701 | 109.8 | 129.8 | 17.2 | 0.0350 |
| Ti10V-31-1 | --- | 0.01024 | 135.7 | 136.7 | 13.0 | 0.0286 |
| -2 | --- | 0.01052 | 119.8 | 133.1 | 14.6 | 0.0214 |
| -3 | --- | 0.01037 | 121.5 | 125.4 | 14.5 | 0.0127 |
| Ti10V-34 | 6.4 | 0.00690 | 139.9 | 144.9 | 19.3 | 0.0102 |
| Ti10V-35 | 5.1 | 0.00731 | (a) | 134.7 | (a) | (a) |

---

(a) Load-strain curve not suitable for determining property.

## 4.3 Carbon Filament Reinforced Al Alloy Composites

### 4.3.1 Camphene Aligned, Liquid Phase Hot Pressed Composites

Composites of 2024 Al alloy, as pressed and in the T6 heat treated condition, with graphite fiber contents of 40, 30, and 20 v/o, were prepared as described in section 2.2.3. Two types of graphite fibers, Thornel 75 and Modmor Type 1, were initially scheduled for evaluation, but only one composite sample could be prepared with the Modmor fibers of quality comparable to that of the Thornel samples.

Tensile specimens machined from the composite samples were tested by loading the specimen to full scale on the low load range, unloading, switching to the next higher load range, and repeating until failure occurred. The results of the tensile tests are presented in Tables IV and V.

In most cases the elastic modulus was found to increase after the initial loading, possibly indicating that the efficiency of load transfer to the fibers from the matrix may have been improved by microstraining of the matrix at the bond. The measured increase in elastic modulus produced by 20 and 30 v/o reinforcement was approximately 75% of the value predicted by the law of mixtures, while that for 40 v/o reinforcement was less than 67%.

Ultimate tensile strengths of the composite specimens were lower than the matrix strengths of approximately 50 kpsi for the as-pressed and 60 kpsi for the T6 heat-treated condition. Failure strains of the composites were also reduced, the 40 v/o specimens having the lowest values.

Heat treating the matrix to the T6 condition increased the ultimate tensile strength and the failure strain of the composites in proportion to the increase in these properties for the matrix in the T6 condition.

The one Modmor composite, C-38, tested in the as-pressed condition, had approximately twice the ultimate tensile strength and three times the strain to failure of the comparable 40 v/o as-pressed Thornel composite, C-28. Metallographic analysis of the fractured tensile specimens indicated that the principal causes for the low tensile strength were fiber damage and low strength of the fiber-matrix bond. Evidence of fiber damage can be seen in figure 7. Initially, the Thornel 75 fibers were 1/2 in. long as received. After boiling in water to remove the sizing and ultrasonic dispersion, the fibers were reduced in length as shown in figure 7(a).

## TABLE IV

## MECHANICAL PROPERTIES OF 2024 Al/GRAPHITE FIBER COMPOSITES

| | | | | Tensile Properties | | |
|---|---|---|---|---|---|---|
| Test Specimen No. | Fiber Content | Matrix Heat Treatment | Cross-Sectional Area | Ultimate Strength | Elastic Modulus | Total Strain to Failure |
| | v/o | | in.$^2$ | kpsi | Mpsi | in./in. |
| | | Longitudinal | | | | |
| C-27-1 | 40 | T6 | 0.01336 | 28.4 | 26.0 | 0.00138 |
| -2 | " | " | 0.01268 | 28.8 | 22.4 | 0.00146 |
| -3 | " | " | 0.01332 | 27.0 | 27.8 | 0.00107 |
| C-28-1 | 40 | None | 0.01458 | 23.7 | 33.2 | 0.00077 |
| -2 | " | " | 0.01395 | 21.5 | 31.0 | 0.00085 |
| -3 | " | " | 0.01466 | 19.8 | 30.7 | 0.00085 |
| C-30-1 | 30 | T6 | 0.01793 | 35.7 | 24.9 | 0.00199 |
| -2 | " | " | 0.01850 | 37.0 | 21.7 | 0.00214 |
| -3 | " | " | 0.01814 | 38.3 | 22.5 | 0.00230 |
| C-31-1 | 30 | None | 0.01795 | 32.1 | 23.9 | 0.00154 |
| -2 | " | " | 0.01845 | 33.1 | 23.4 | 0.00185 |
| -3 | " | " | 0.01855 | 34.5 | 23.3 | 0.00185 |
| C-32-1 | 20 | T6 | 0.01700 | 35.3 | 18.4 | 0.00322 |
| -2 | " | " | 0.01665 | 36.6 | 16.0 | 0.00426 |
| -3 | " | " | 0.01690 | 36.4 | 17.4 | 0.00337 |
| C-33-1 | 20 | None | 0.01797 | 30.1 | 17.4 | 0.00316 |
| -2 | " | " | 0.01807 | 30.0 | 17.8 | 0.00309 |
| -3 | " | " | 0.01748 | 29.5 | 17.3 | 0.00293 |
| C-38-1 | 40* | None | 0.01316 | 43.7 | 29.9 | 0.00172 |
| -2 | " | " | 0.01316 | 44.8 | 28.7 | 0.00253 |
| -3 | " | " | 0.01272 | 51.1 | 26.1 | 0.00260 |
| | | Transverse | | | | |
| C-36-1 | 40 | T6 | 0.01410 | 4.82 | 2.57 | 0.00222 |
| -2 | " | " | 0.01400 | 4.57 | 2.10 | 0.00260 |
| -3 | " | " | 0.01370 | 5.25 | 2.90 | 0.00230 |
| C-36-1 | 30 | T6 | 0.01780 | 7.42 | 3.34 | 0.00291 |
| -2 | " | " | 0.01790 | 7.15 | 3.02 | 0.00300 |
| -3 | " | " | 0.01695 | 7.20 | 3.97 | 0.00215 |
| C-37-1 | 20 | T6 | 0.01642 | 12.06 | 5.60 | 0.00299 |
| -2 | " | " | 0.01642 | 11.00 | 4.50 | 0.00291 |
| -3 | " | " | 0.01614 | 10.65 | 4.39 | 0.00299 |

* Modmor fibers; all others Thornel.

## TABLE V

## ELASTIC MODULUS OF 2024 Al/GRAPHITE FIBER COMPOSITES UNDER SUCCESSIVELY INCREASED LOADS

| Test Specimen No. | Fiber Content v/o | Modulus of Elasticity, Mpsi, Over Load Range | | |
|---|---|---|---|---|
| | | 0-200 lb | 0-500 lb | 0-1000 lb |
| C-27-1 | 40 | 25.7 | 26.0 | |
| -2 | 40 | ** | 22.4 | |
| -3 | 40 | 21.8 | 27.8 | |
| C-28-1 | 40 | 29.6 | 33.2 | |
| -2 | 40 | 27.3 | 31.0 | |
| -3 | 40 | 25.3 | 30.7 | |
| C-30-1 | 30 | 12.3 | 23.0 | 24.9 |
| -2 | 30 | 22.0 | 21.2 | 21.7 |
| -3 | 30 | 15.6 | 20.2 | 22.5 |
| C-31-1 | 30 | 22.6 | 22.8 | 23.9 |
| -2 | 30 | 20.1 | 22.2 | 23.4 |
| -3 | 30 | 18.4 | 21.3 | 23.3 |
| C-32-1 | 20 | 19.7 | 18.6 | 18.4 |
| -2 | 20 | 15.7 | 15.9 | 16.0 |
| -3 | 20 | 16.1 | 17.6 | 17.4 |
| C-33-1 | 20 | 14.7 | 17.0 | 17.4 |
| -2 | 20 | 15.6 | 18.3 | 17.8 |
| -3 | 20 | 18.5 | 18.5 | 17.3 |
| C-38-1 | 40* | 26.1 | 29.5 | 29.9 |
| -2 | 40* | 21.1 | 25.8 | 28.7 |
| -3 | 40* | 22.8 | 24.7 | 26.1 |

---

* Modmor fibers; all others Thornel.

**Load-strain curve unsuitable for determination of modulus.

Further reduction in length of the brittle fibers may have occurred during the camphene extrusion. Some fiber breakage also occurs during hot pressing because of contacts between crossed filaments and interference between filaments and solid matrix particles. Representative examples of the final fiber lengths are shown in figure 7(b), (c), and (d).

Evidence that the bond strength was low can be seen in figure 8, which shows the fibers projecting from a tensile fracture face after pullout from the mating half of the tensile specimen. This behavior was observed in all the longitudinal tensile tests. Fiber pullout also occurred frequently in the preparation of longitudinal metallographic sections. The longitudinal sections in figures 9, 10, 11, and 12, for example, show many voids while the absence of voids in the transverse sections of the same tensile specimens, also shown in these figures, indicates the low porosity of the original specimens.

Failure at the fiber-matrix interface was indicated by the low tensile strengths, and also by the presence of cracks leading away from the transverse faces of fracture and along the longitudinal fiber interfaces. Such a crack is shown in figure 13.

This observation raised the possibility that the fibers may not have been completely surrounded by the metal matrix, particularly in areas of high fiber concentration, leaving some fiber surfaces in direct contact. Extensive metallographic studies of the 40 v/o composite specimens verified the condition of fiber-to-fiber contact. Shown in figure 14 are two typical examples of the fiber contact problem. The Thornel fibers shown in figure 14(a) appear to have more points of contact, because of their smaller size and irregular surface, than the Modmor fibers shown in figure 14(b); this condition, therefore, may have contributed to the reduction of tensile strength in the Thornel samples.

### 4.3.2 Hot Extruded 2024 Al/C Composites

Radiography of the two extrusions revealed no internal defects. A layered appearance, similar to the rings in a cross section of a tree trunk, and fine porosity were visible in the transverse section (Figure 15). The ring structure observed in the extrusion apparently was due to inhomogeneity in the green bodies from which the extrusion billets were consolidated.

The extent of reduction of the fiber aspect ratio by breakage during the extrusion process can be seen in the longitudinal section in figure 15. It is estimated that the $\ell/d$ ratio is reduced from an average of about 1000 to the order of 10 by extrusion. The breakdown of the fibers, and possibly also poor bonding, prevented the material from acting effectively as reinforcement, and the mechanical properties of the samples (Table VI) are poor. The specimens had ultimate tensile strengths ranging from 26.2 to 39.5 kpsi and elastic moduli ranging from 11.2 to 16.2 Mpsi. Following these results, no further samples were prepared by hot extrusion.

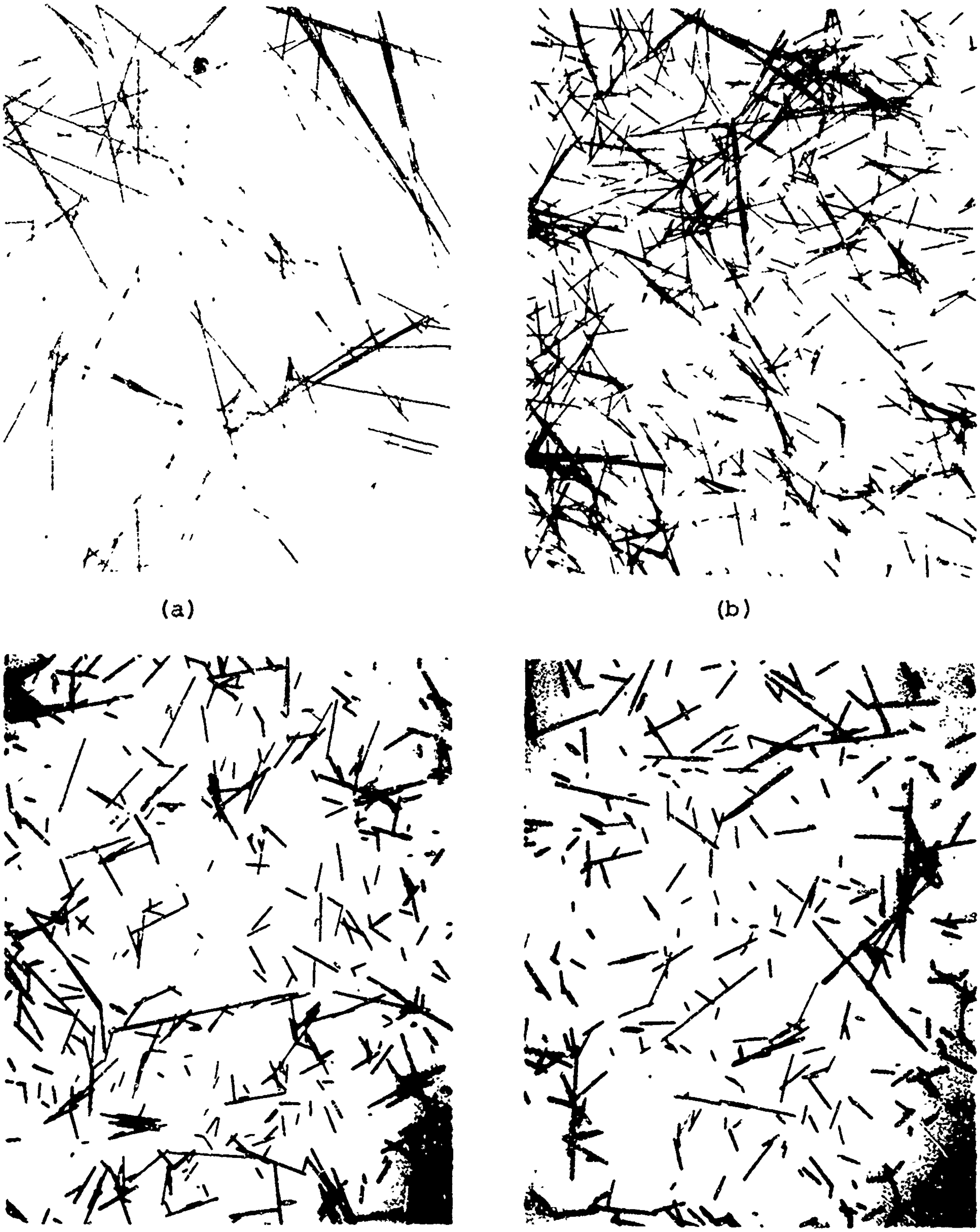

(a) (b)

(c) (d)

Figure 7. Thornel 75 graphite fibers (X50) after (a) ultrasonic dispersion, and after recovery by dissolving the matrix from broken tensile specimens containing (b) 40 v/o, (c) 30 v/o, and (d) 20 v/o fibers.

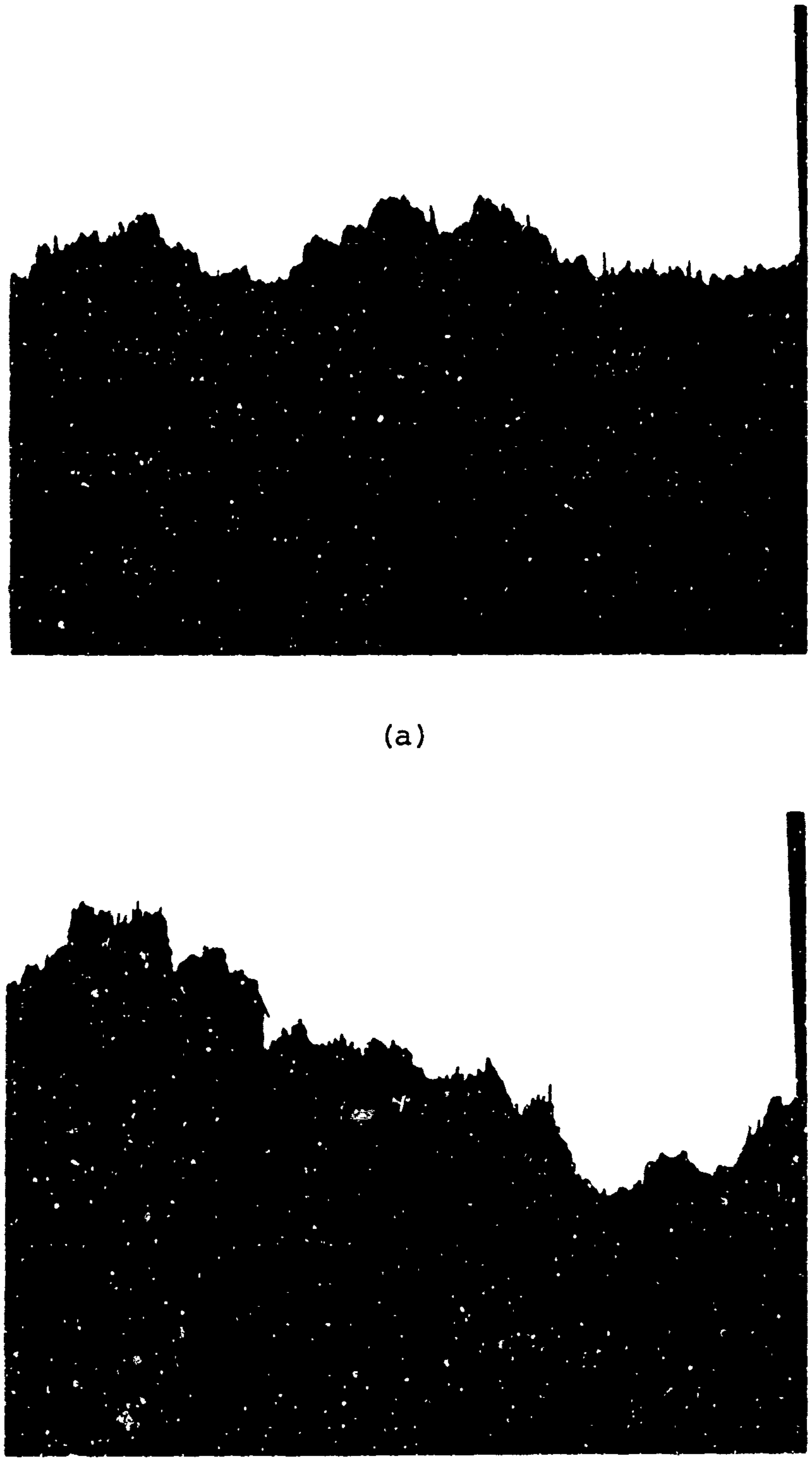

(a)

(b)

Figure 8. Fiber pullout in fracture faces of 2024 Al/graphite fiber composites (X50): (a) 40 v/o Thornel 75 fiber, (b) 40 v/o Modmor fiber.

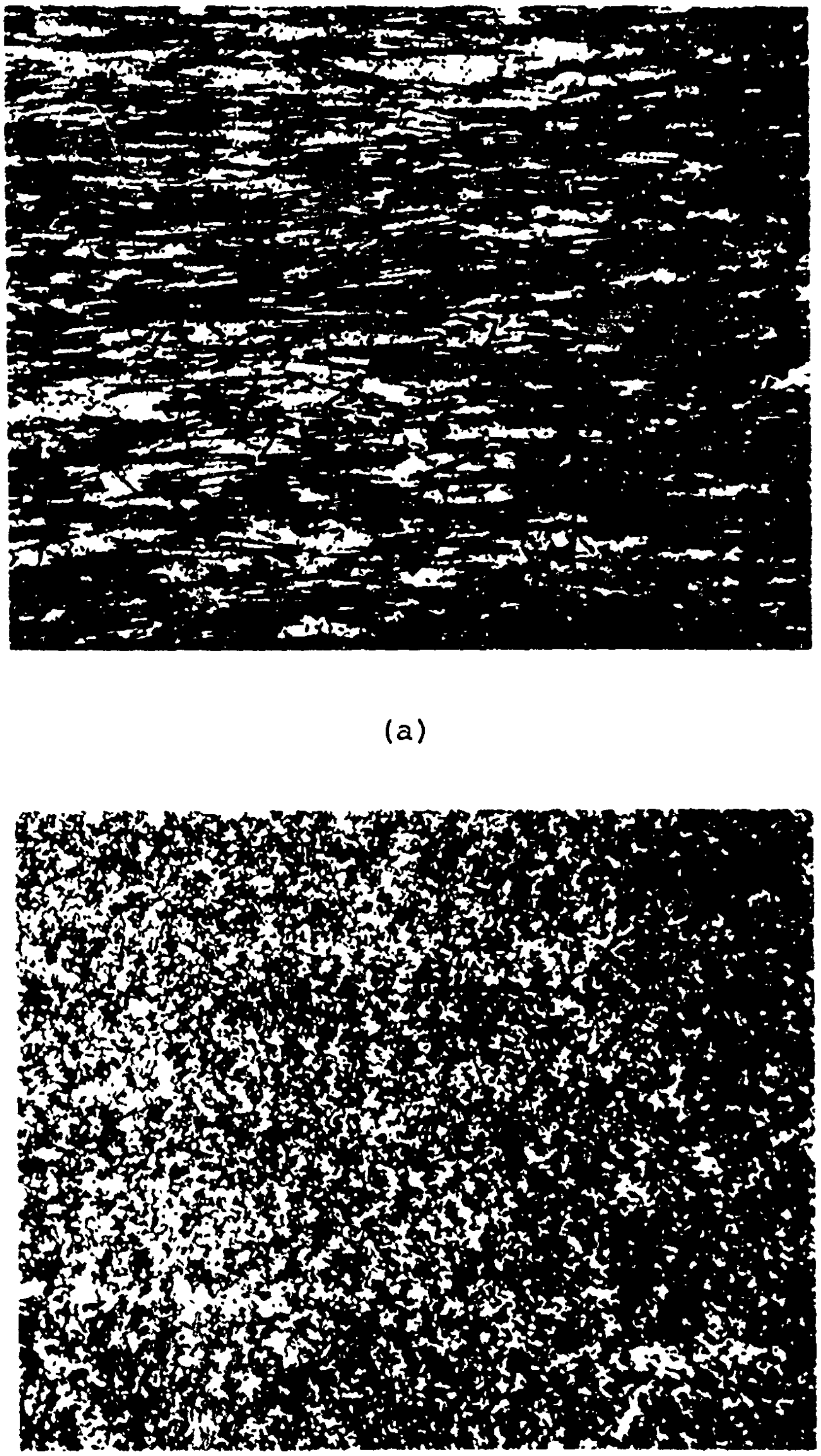

Figure 9. Representative sections of 2024 Al/40 v/o Thornel 75 fiber composite (X75): (a) longitudinal and (b) transverse.

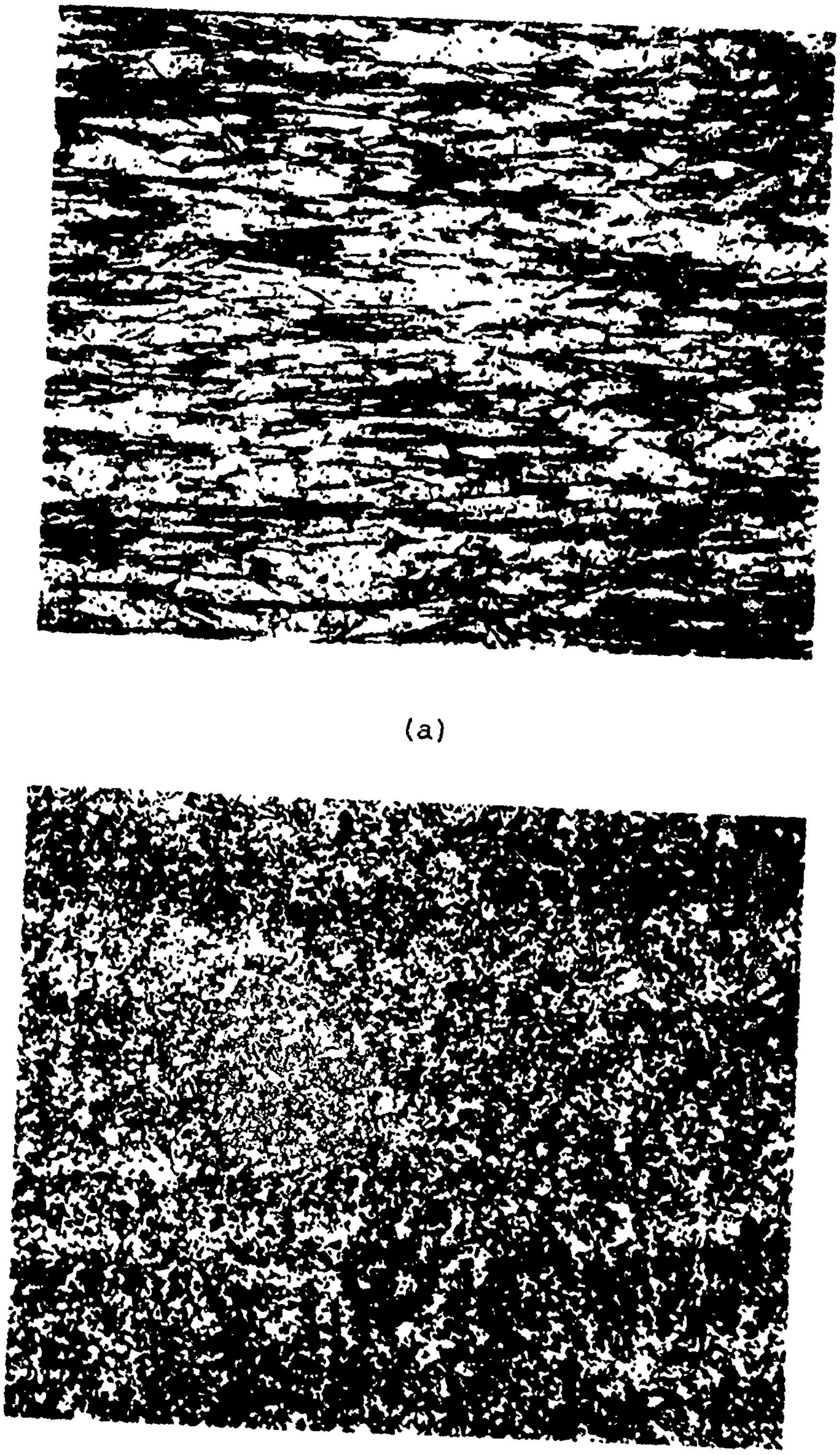

Figure 10. Representative sections of a 2024 Al/30 v/o Thornel 75 fiber composite (X75): (a) longitudinal and (b) transverse.

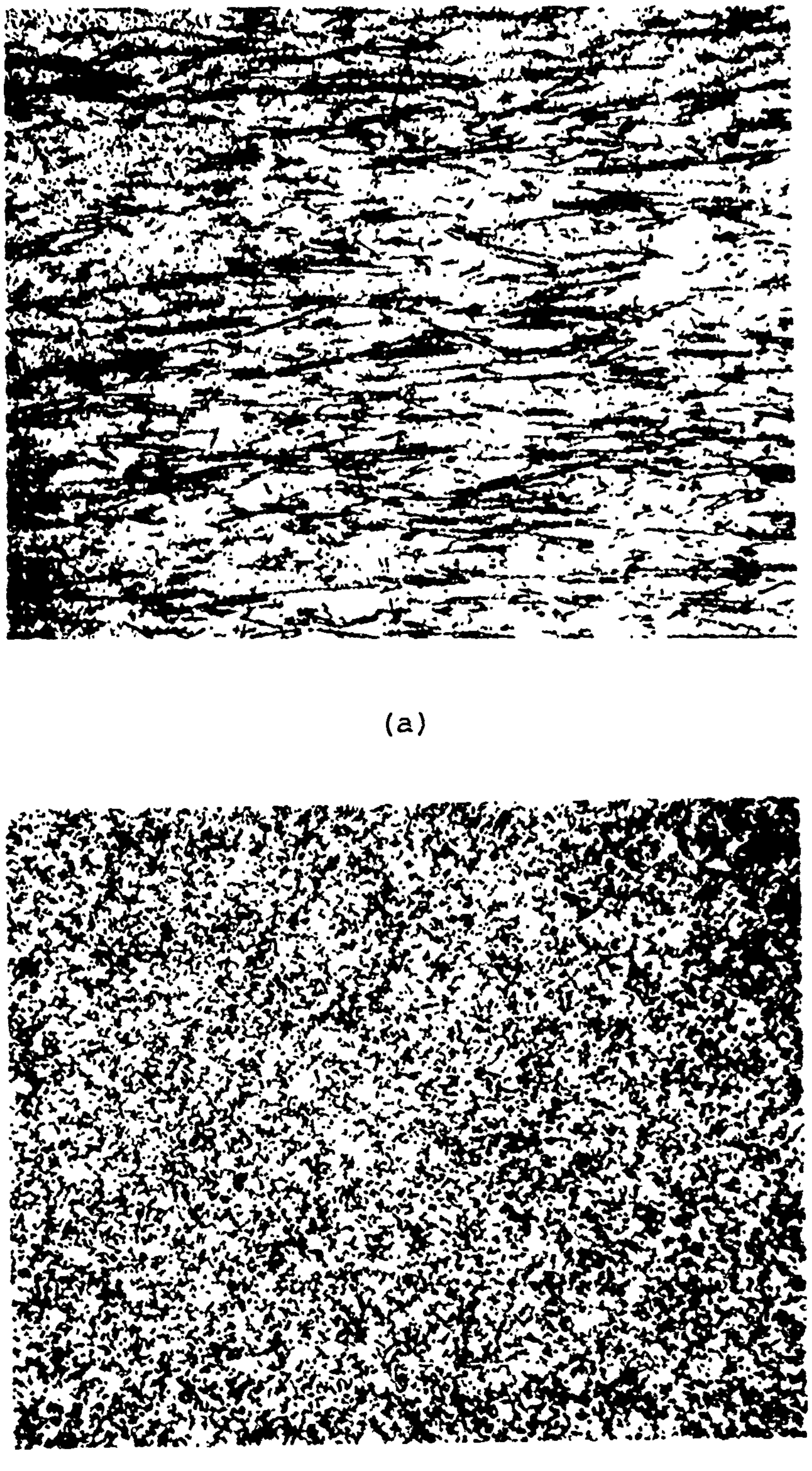

(a)

(b)

Figure 11. Representative sections of a 2024 Al/20 v/o Thornel 75 fiber composite (X75): (a) longitudinal and (b) transverse.

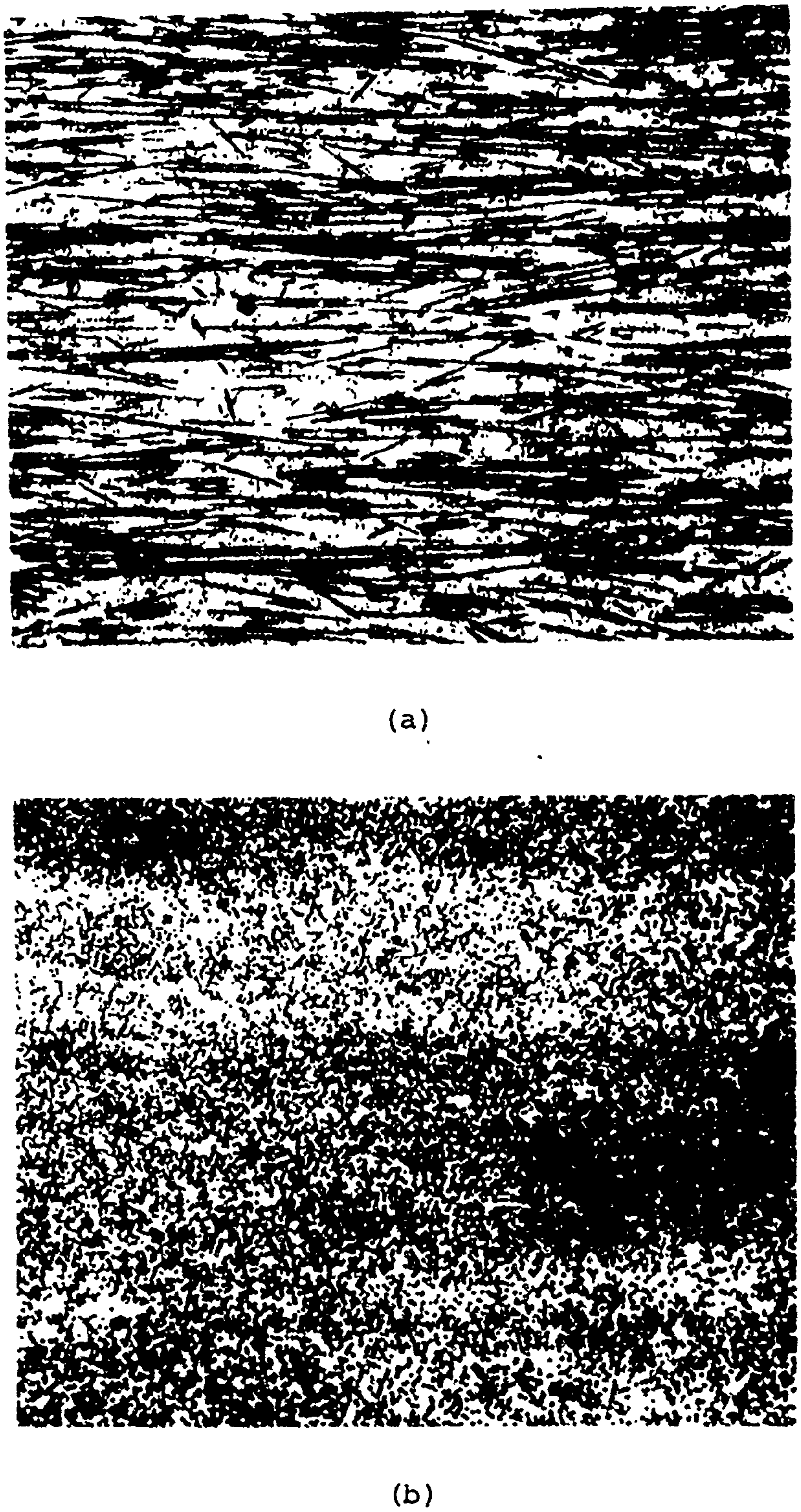

Figure 12. Representative sections of a 2024 Al/40 v/o Modmor fiber composite (X75): (a) longitudinal and (b) transverse.

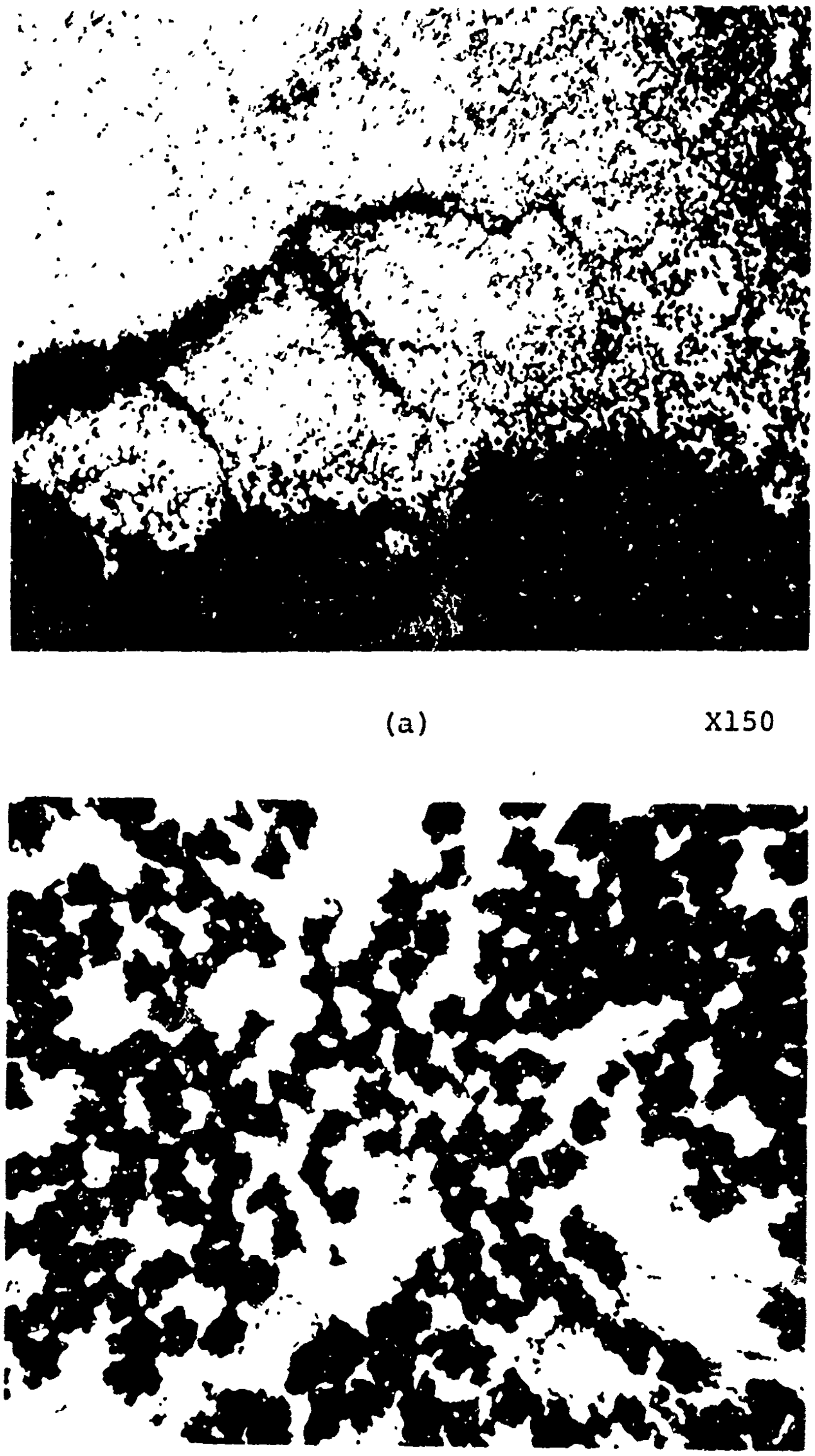

(a) X150

(b) X750

Figure 13. Crack proceeding from fracture face in (a) transverse plane and (b) along connecting fibers at the fiber-matrix interface.

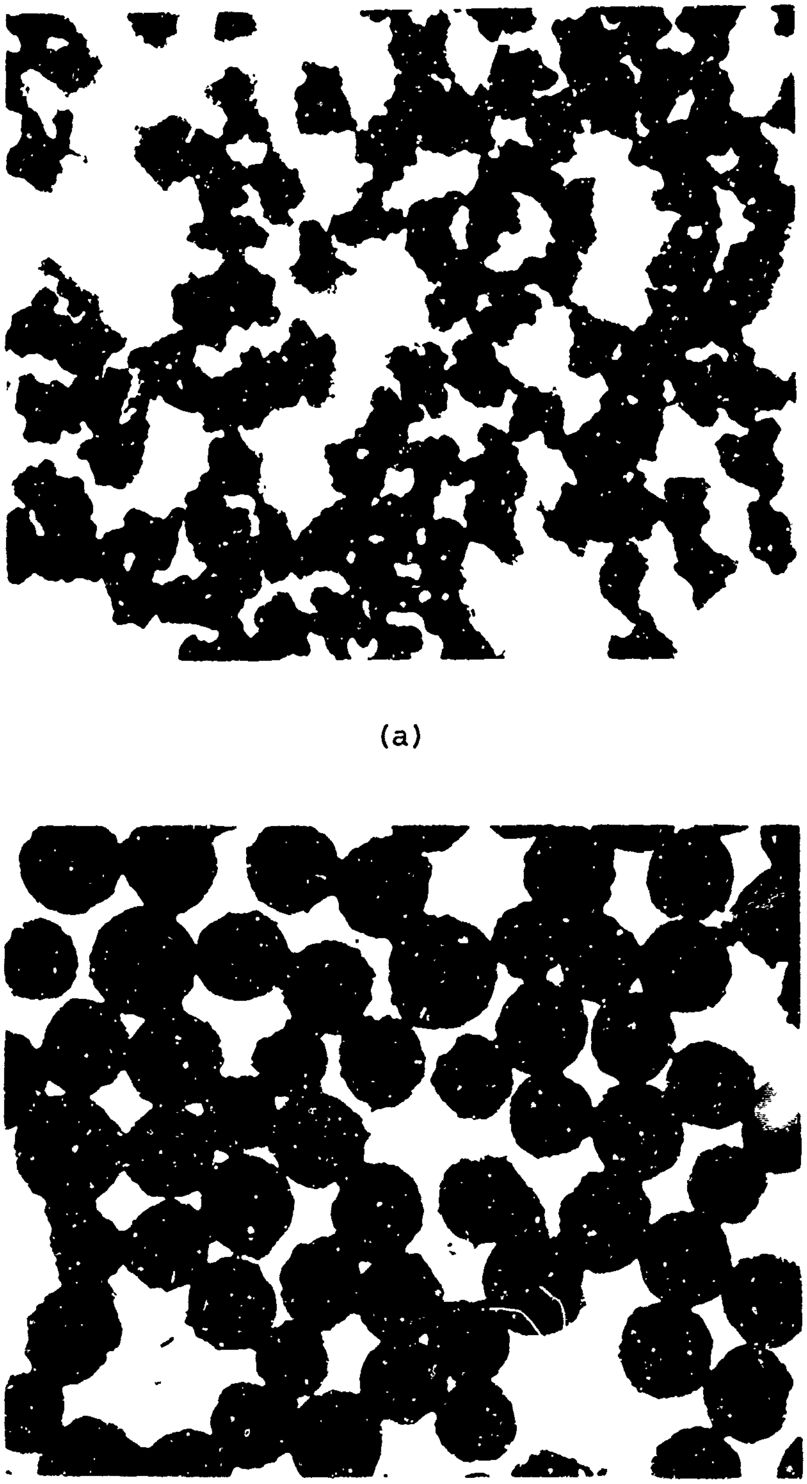

(a)

(b)

Figure 14. Fiber-to-fiber contact in 2024 Al/40 v/o graphite fiber composites (X1500): (a) Thornel 75 and (b) Modmor Type 1.

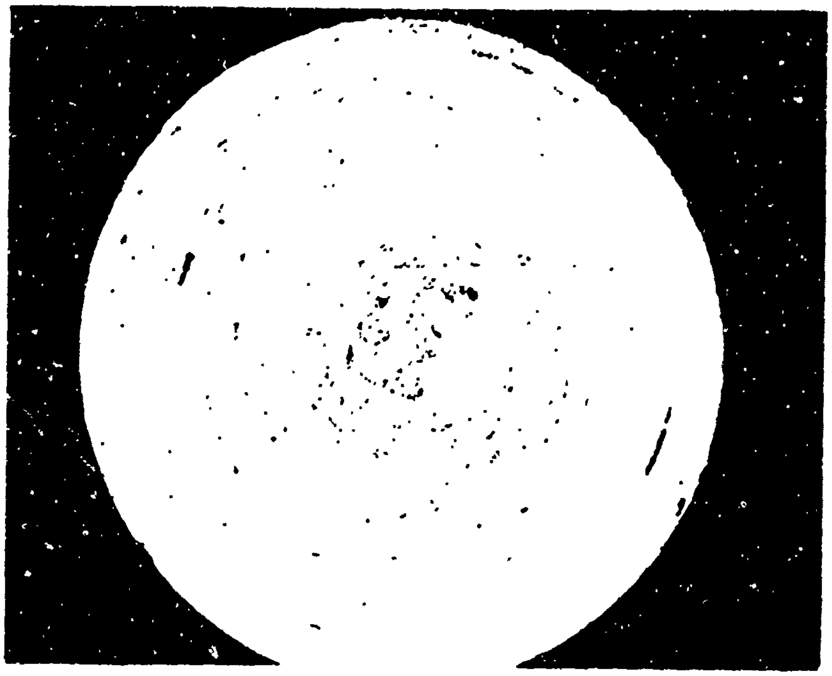

Transverse 11X

Longitudinal 250X

Figure 15. Sections of hot extruded 2024 Al/20 v/o C composite

## TABLE VI

## MECHANICAL PROPERTIES OF HOT EXTRUDED 2024 Al/20 v/o C DISCONTINUOUS FILAMENT COMPOSITES

| Sample No. | Yield Strength kpsi | Ultimate Strength kpsi | Elastic Modulus Mpsi | Strain to Failure % |
|---|---|---|---|---|
| C234-3 | -- | 33.6 | 11.5 | 0.397 |
| -5 | -- | 26.2 | 11.2 | 0.280 |
| -6 | 37.9 | 38.1 | 12.6 | 0.508 |
| C567-4 | -- | 29.9 | 12.8 | 0.290 |
| -5 | -- | 33.8 | 12.8 | 0.390 |
| -7 | -- | 38.7 | 14.2 | 0.413 |
| -8 | -- | 39.5 | 16.2 | 0.275 |

## SECTION 5

## CONCLUSIONS

A thin CeS coating may deteriorate rather rapidly when heated, even in vacuum, owing to reaction with residual oxygen. A coating on the order of 1 μm thick has been shown to persist on titanium through hot pressing at 6000 psi and 1000°C for 2 hr. A CeS coating appears effective in retarding the reaction of SiC fibers with a titanium matrix up to 930°C (1700°F). A composite reinforced with CeS-coated SiC fibers behaved satisfactorily in transverse tensile tests, with no evidence of fiber splitting. Evaluation of the structural performance of the CeS coating will require testing and examination of longitudinal tensile specimens.

Consolidation of Ti-10V and Ti-30V by activated pressure sintering of the hydride powders can be effected at 800°C in 1 hr. Reaction of SiC fibers with matrices consolidated in this way is much less rapid than with pure titanium, the reaction zone being indistinguishable by microscopy in Ti-30V after 3 hr and at most barely visible (less than 1 μm) in Ti-10V.

The SiC fiber reinforcement of the Ti-V alloys increased the modulus in the expected proportion to the fiber content. Strength was significantly improved in the Ti-10V composite, but was significantly less in the Ti-30V composite than in the corresponding unreinforced alloy. Further study of the Ti-10V composite, at least, appears desirable.

The technique of sedimentation in camphene produces homogeneous, well dispersed green cakes of metal powder/fiber mixture, but the 2024 Al/graphite composites resulting from liquid-phase hot pressing of these green bodies show fiber-fiber contact, porosity, low bond strength, and fiber pullout in tensile tests due to incomplete penetration and wetting by the matrix.

Hot extrusion of 2024 Al/graphite filament composites reduced the aspect ratio ($\ell/d$) of the fibers severely and yielded material of unsatisfactory strength and modulus. The process is therefore considered unsuitable for the composites.

# SECTION 6

# FUTURE WORK

## 6.1 Aluminum Alloy/Discontinuous Fiber Composites

By means of liquid phase hot pressing techniques previously developed, Al alloy/discontinuous fiber composites will be consolidated from green bodies aligned by the camphene extrusion process. The aluminum alloys which will be used as matrices are 2024 and a 7000 series Al alloy. Chopped carbon filaments and β-SiC whiskers will be utilized as the reinforcement.

Sufficient amounts of 2024 Al/25 v/o β-SiC composites will be prepared to provide replicate samples for elevated temperature tensile testing, low cycle-high stress fatigue testing, and if applicable, tensile impact testing. In all cases, testing will be performed on composites with both longitudinal and transverse fiber orientation. Elevated temperature tensile testing will be performed at three temperatures to be selected between room temperature and 800°F. Low cycle-high stress fatigue testing will be performed at room temperature and at an elevated temperature to be selected.

High strength 7000 series Al alloy composites reinforced with 25 v/o and 40 v/o β-SiC whiskers will be consolidated and evaluated by metallography and mechanical testing. It is expected that the use of a 7000 series alloy, with its increased yield and tensile strengths, will result in a 25 v/o whisker composite with a tensile strength approaching 250,000 psi. The advent of a precision powder classification process, which allows the collection of very fine powders such as -600 mesh, has improved the feasibility of consolidating a sound 40 v/o whisker composite, since a better match may be obtained between the fiber and powder size in the green body.

The development effort initiated in this program for the consolidation and characterization of Al alloy/discontinuous C fiber composites will be continued. In the work contemplated, the coating of discontinuous carbon filaments with copper and nickel by electroless plating and/or chemical vapor deposition will be utilized to improve fiber distribution in the composites by improving the wetting characteristics and the bonding of the filaments. Composites with 25 to 40 v/o discontinuous carbon filaments will be consolidated. These will be evaluated by room temperature mechanical testing and, if warranted, by elevated temperature mechanical testing to 800°F as well as by metallographic examination.

## 6.2 Titanium Alloy/Boron and/or Borsic Composites

Boron and/or Borsic filament reinforced composites will be fabricated by two techniques, activated pressure sintering of Ti-10V and diffusion bonding of a Titanium-6Al-4V alloy which is superplastic at the consolidation temperature. The consolidation of Ti-10V matrix composites will be based upon the parameters established in the current program. A CeS coating may be used on the filaments if the results of metallographic and mechanical testing of composites so indicate.

Based upon the results of Backofen, et al.,(4) and the results of in-house experiments with superplastic ternary Ni-Cr-Fe alloys, ARTECH intends to investigate the consolidation of boron and Borsic filament Ti-6Al-4V composites by vacuum hot pressing in the temperature range in which the alloy is superplastic. Initially, the layup of the composites for pressing will consist of one layer of filaments placed in grooves in the titanium alloy sheets. Orientation of the fibers will be transverse to the loading direction. Test specimens approaching 1/2 in. wide and 3-1/2 in. long, with fibers protruding from the 2-in. gauge section, will be consolidated. Both uncoated and CeS-coated filaments will be utilized in this part of the program. Measurements of the densities, metallographic examination of the composites, and room temperature tensile tests of the samples will be performed to monitor the effectiveness of the consolidation process as well as to determine the effectiveness of bonding. If evaluation of the samples fabricated in the manner discussed above is favorable, composite test samples with longitudinal and transverse fiber orientation will be prepared containing at least 30% fibers by volume. The samples so produced will be tensile tested at room temperature and examined metallographically.

# SECTION 7

# TECHNOLOGICAL FORECAST FOR LIGHT METAL/DISCONTINUOUS FIBER REINFORCED COMPOSITES

## 7.1 Background

A discontinuous fiber composite usually contains a strong, brittle, aligned phase distributed in a softer matrix alloy. This discontinuous fiber reinforces the composite by carrying the load transferred by matrix deformation. The matrix prevents formation of a continuous brittle path through the composite, binds and protects the fibers, and transfers stress between the fibers.

## 7.2 Present Status

Reinforcement of light metal alloys with discontinuous fibers has presently been limited to aluminum, magnesium, and titanium alloys reinforced with chopped graphite fibers, sapphire, $\alpha$-SiC, and $\beta$-SiC whiskers. The best aluminum alloy whisker composite, which was prepared under Navy sponsorship, has a compressive strength of 250,000 psi and elastic modulus in tension of $27.0 \times 10^6$ psi with 25 volume percent $\beta$-SiC whiskers. During the past year, research was conducted on the development of a protective coating for filaments in titanium matrices. Results of the work indicated that a cerium monosulfide (CeS) coating appears effective as a diffusion barrier in titanium matrix composites. However, further work is required to determine the bond strength attained between the coating and fiber and the matrix and the coating. In addition, composites prepared from Ti-10V reinforced with SiC filaments and consolidated by activated pressure sintering show promise.

## 7.3 Forecast

The role of composites in future materials technology will be extensive. Continuous and discontinuous fiber reinforced composites will provide highly efficient special-purpose materials with properties that are not currently available in conventional materials. Metal matrices will be increasingly employed for higher strength and higher temperature applications. Continuous fiber reinforced composites will be used in applications requiring highest strengths in which cost is not a limiting factor. Discontinuous fiber metal-matrix composites will become available for commercial application later than continuous fiber composites because their development funding has been more restricted. Discontinuous fiber metal-matrix composites may be fabricated into intricate shapes and are not limited by required lamination or winding processes peculiar to composites reinforced with continuous filaments. Discontinuous fiber reinforced composites will provide strength and stiffness and maintain these properties at elevated temperatures. It is anticipated that applications of the discontinuous fiber composites will be those which require the unique properties of these materials but in which cost is also a factor.

It is anticipated that high strength graphite fibers and β-SiC whiskers, which are several times more expensive at present but under intensive commercial development, will be the primary discontinuous fibers used for reinforcement. The mechanical properties of composites as anticipated in composites of the future are shown as a function of time in figure 16. The values shown are those for the best aluminum alloys reinforced by currently available whiskers, which may approach theoretical maximum strength values, or high strength fibers of graphite or other polycrystalline materials that will become available. It is interesting to note that points (1) and (2) which are marked on the graphs represent two composites that have been produced since the preparation of that section of the property forecast curves. The strength and modulus of material produced have exceeded the predicted values up to 1972. The anticipated increased uses of these materials, represented by increasing production and decreasing cost, are similarly extended in figure 17 from previous forecast curves. Owing to reduction of Government support, the cost reductions and production increases have not occurred for these materials as rapidly as predicted.

## 7.4 Operational Implications

With improvement in fiber quality, lower cost, and continued progress in the development of fabrication techniques, discontinuous fiber light-metal composites are expected to be utilized in numerous applications requiring materials tailored to the job. Parts of complex configuration that require high stiffness/density and strength/density ratios are applications of immediate interest for these composites. Selective reinforcement will make these materials even more effective in the future for such possible applications as bearing surfaces, multi-hardness armor, and erosion-resistant components.

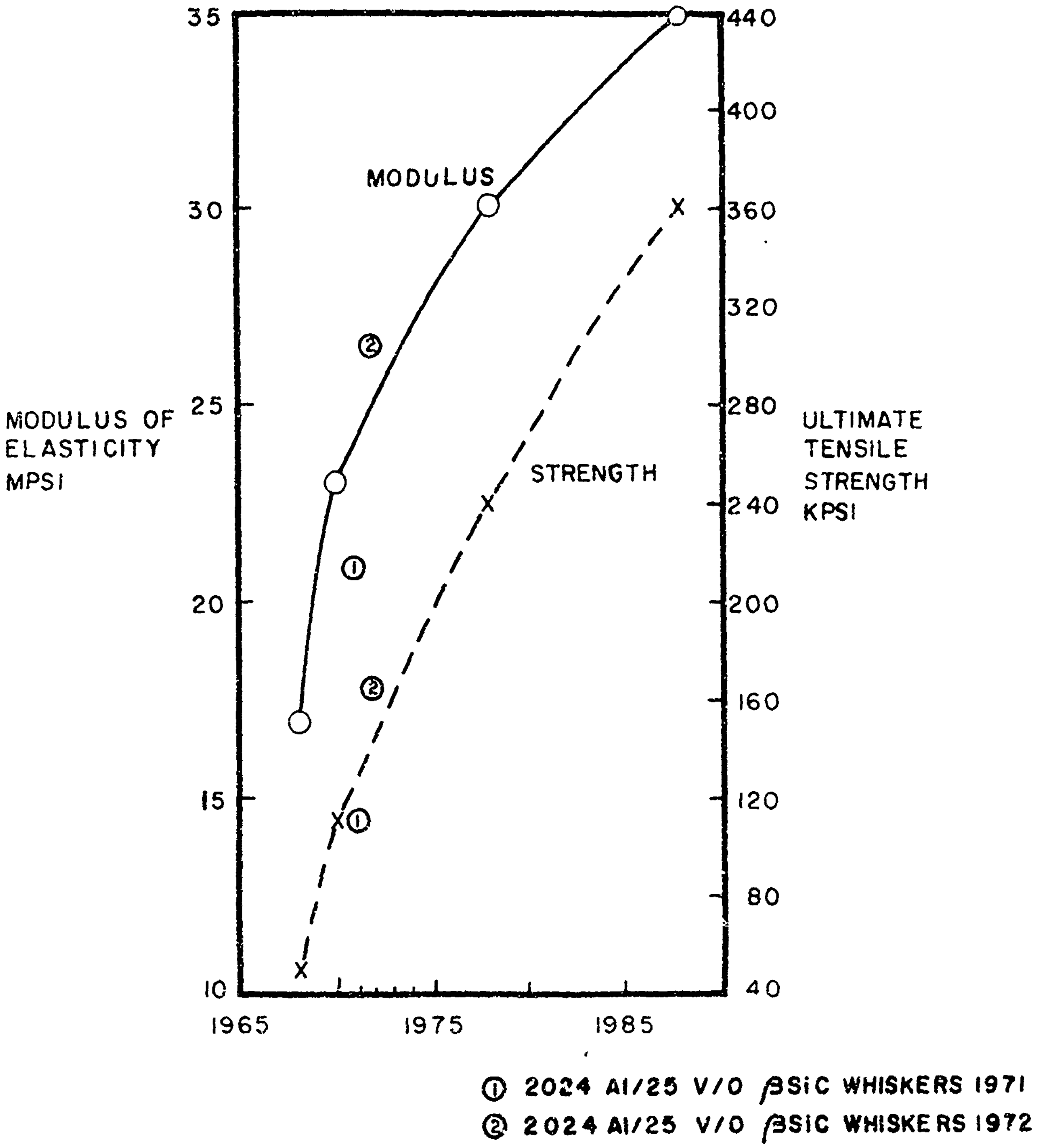

Figure 16. Predicted improvement in mechanical properties of 20 v/o discontinuous fiber light metal composites through 1990.

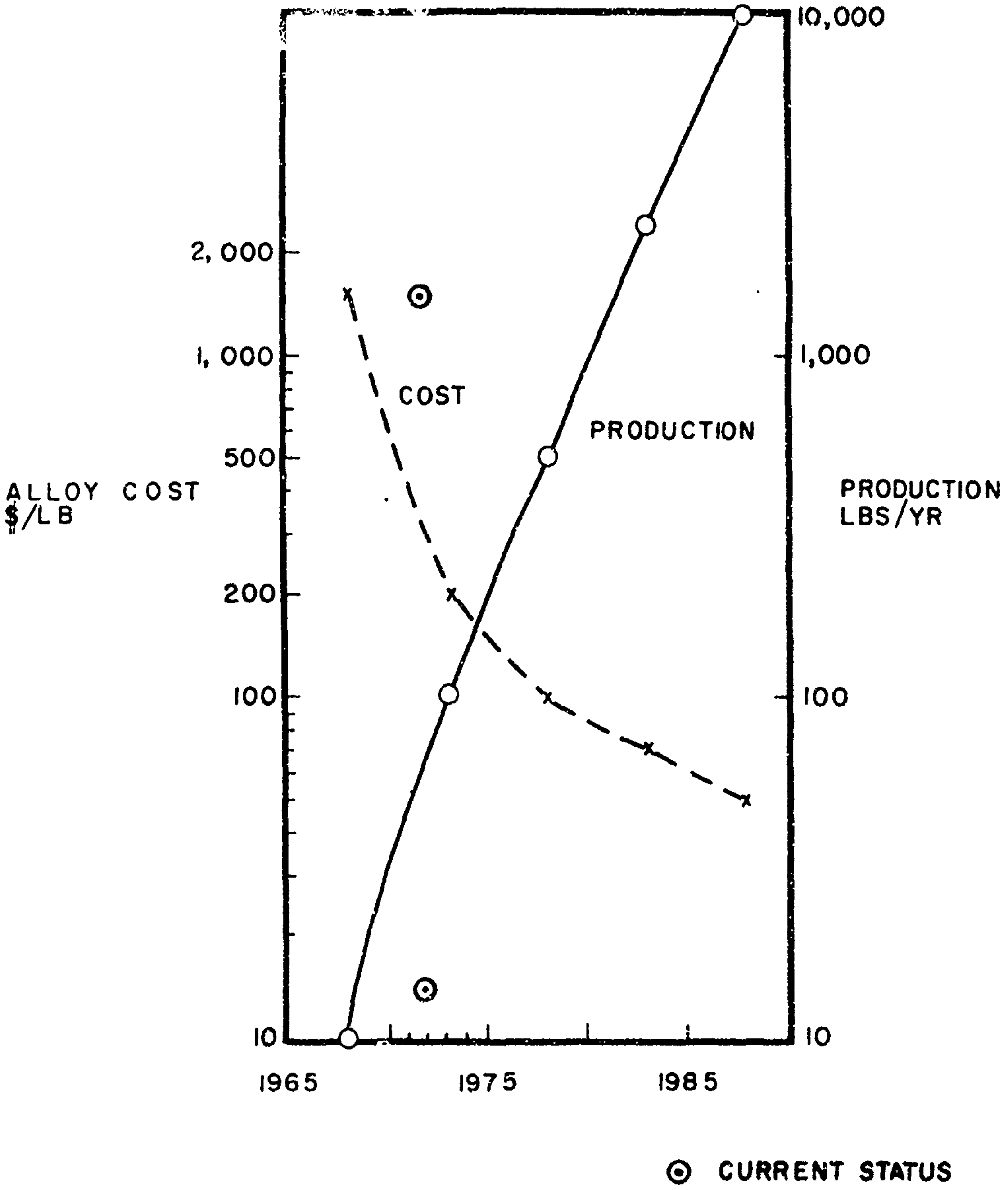

Figure 17. Predicted production and cost of discontinuous fiber reinforced composites through 1990.

## REFERENCES

(1) R. A. Hermann, P. J. Lare, F. Ordway, and H. Hahn, "Whisker Reinforced Metals", Final Report, Contract N00017-69-C-4429, ARTECH CORP., Falls Church, Va. (1970).

(2) L. M. Litz and J. M. Blocher, Jr., "Sulfides", Chapter 13, pp. 431-54 in "High-Temperature Materials and Technology", I. E. Campbell and E. M. Sherwood, eds., John Wiley, New York (1967).

(3) H. Schuerch, "Contribution to the Micromechanics of Composite Materials--Stresses and Failure Mechanisms Induced by Inclusions", NASA Contractor Report CR-582 (1966).

(4) W. A. Backofen and W. W. Wilkening, "Deformation Processing of Anisotropic Metals", Final Technical Report, Contract N00019-70-C-0071, Massachusetts Institute of Technology, Cambridge, Mass. (1970).